Acta Cryst A FOUNDATIONS ADVANCES

ISSN 2053-2733

Unique atom hyper-kagome order in $Na_4Ir_3O_8$ and in low-symmetry spinel modifications

V. M. Talanov,[a]* V. B. Shirokov[b] and M. V. Talanov[c]

[a]South Russia State Polytechnical University (Novocherkassk Polytechnic Institute), 346400 Novocherkassk, Russian Federation, [b]South Scientific Center, Russian Academy of Sciences, 344006 Rostov-on-Don, Russian Federation, and [c]South Federal University, Rostov-on-Don, Russian Federation. *Correspondence e-mail: valtalanov@mail.ru

Received 1 October 2014
Accepted 24 February 2015

Edited by W. F. Kuhs, Georg-August University Göttingen, Germany

Keywords: hyper-kagome order; ordered spinels; enantiomorphic modifications; atom and orbital orders; decagons.

Group-theoretical and thermodynamic methods of the Landau theory of phase transitions are used to investigate the hyper-kagome atomic order in structures of ordered spinels and a spinel-like $Na_4Ir_3O_8$ crystal. The formation of an atom hyper-kagome sublattice in $Na_4Ir_3O_8$ is described theoretically on the basis of the archetype (hypothetical parent structure/phase) concept. The archetype structure of $Na_4Ir_3O_8$ has a spinel-like structure (space group $Fd\bar{3}m$) and composition $[Na_{1/2}Ir_{3/2}]^{16d}[Na_{3/2}]^{16c}O^{32e}{}_4$. The critical order parameter which induces hypothetical phase transition has been stated. It is shown that the derived structure of $Na_4Ir_3O_8$ is formed as a result of the displacements of Na, Ir and O atoms, and ordering of Na, Ir and O atoms, ordering d_{xy}, d_{xz}, d_{yz} orbitals as well. Ordering of all atoms takes place according to the type 1:3. Ir and Na atoms form an intriguing atom order: a network of corner-shared Ir triangles called a hyper-kagome lattice. The Ir atoms form nanoclusters which are named decagons. The existence of hyper-kagome lattices in six types of ordered spinel structures is predicted theoretically. The structure mechanisms of the formation of the predicted hyper-kagome atom order in some ordered spinel phases are established. For a number of cases typical diagrams of possible crystal phase states are built in the framework of the Landau theory of phase transitions. Thermodynamical conditions of hyper-kagome order formation are discussed by means of these diagrams. The proposed theory is in accordance with experimental data.

1. Introduction

Structures in the spinel family AB_2X_4 have held the interest of scientists over many years and continue to attract a wider interest because of their important physical properties. Spinel compounds exhibit a wide spectrum of magnetic and electric properties (Krupichka, 1976). In particular some compounds are superconductors (Johnston *et al.*, 1973; Robbins *et al.*, 1967). Among spinels there are multiferroics (Ederer & Spaldin, 2004; Yamasaki *et al.*, 2006; Torgashev *et al.*, 2012; Gorjaga *et al.*, 1990), numerous materials for electrodes in chemical current sources (Thackeray, 1997; Ezikian *et al.*, 1988; Talanov *et al.*, 2007), crystals with superionic conductivity (Kanno *et al.*, 1981, 1987, 1992; Lutz *et al.*, 1985, 1989, 1997) and materials with other unique properties (Singh *et al.*, 1999; Menyuk *et al.*, 1964; Hastings & Corliss, 1962; Plumier, 1967; Sun *et al.*, 2009, 2010; Hemberger *et al.*, 2005; Catalan & Scott, 2007).

The unusual physical properties of spinels are due, to a great extent, to the fundamental geometric peculiarity of their structure: the octahedral or *B* sublattice of spinels is a frustrated sublattice (Anderson, 1956). Let us explain what that means.

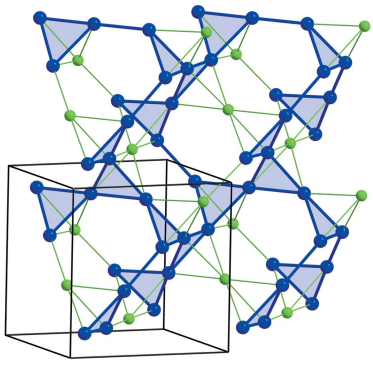

The term 'geometrical frustration' refers to structures with local order, due to the geometry of the lattice. Frustration arises when the geometry of a system allows for a set of degenerate ground states. Such highly degenerate systems are extremely sensitive to thermal and quantum fluctuations, and thus intriguing classical and quantum ground states may emerge *via* 'order by disorder' (Villain *et al.*, 1980; Pati & Rao, 2008). In geometrically frustrated structures, the atoms, spins, orbitals and charge are arranged on a lattice with a triangular motif that prevents them from satisfying all their interactions simultaneously. If there are ions of transition elements in a frustrated lattice, possessing orbital degeneracy of ground electronic states, the physical properties of such a crystal prove to be unusual.

Frustration is a classic topic of chemistry and physics of solids that can be traced back to Linus Pauling's work and the work of others on the structure and entropy of crystalline ice and of other crystals with frozen disorder (Pauling, 1935; Giauque & Stout, 1936). In the case of ice, frustration corresponds to the different ways of orienting the water molecules without changing the energy of the system. Residual configurational entropy of ice was observed experimentally (Giauque & Stout, 1936; Giauque & Ashley, 1933).

In two dimensions, if the triangular plaquettes are arranged in an edge-sharing network they form a triangular lattice, but if in a corner-sharing network they form a kagome lattice. These lattices form the basis for frustrated layered materials such as $SrCr_9Ga_{12}O_{19}$ (Obradors *et al.*, 1988), $KCr_3(OH)_6(SO_4)_2$ (Townsend *et al.*, 1986), $BaSn_2ZnGa_4Cr_6O_{22}$ (Obradors *et al.*, 1988; Ramirez *et al.*, 1990, 1992; Hagemann *et al.*, 2001) and spherical keplerates (Todea *et al.*, 2007). In addition, the spin lattices in $La_4Cu_3MoO_{12}$ (Griend *et al.*, 1999) and $RCuO_{2.66}$ (Nunez-Regueiro *et al.*, 1996) are reported to be identical to the kagome lattice (Pati & Rao, 2008).

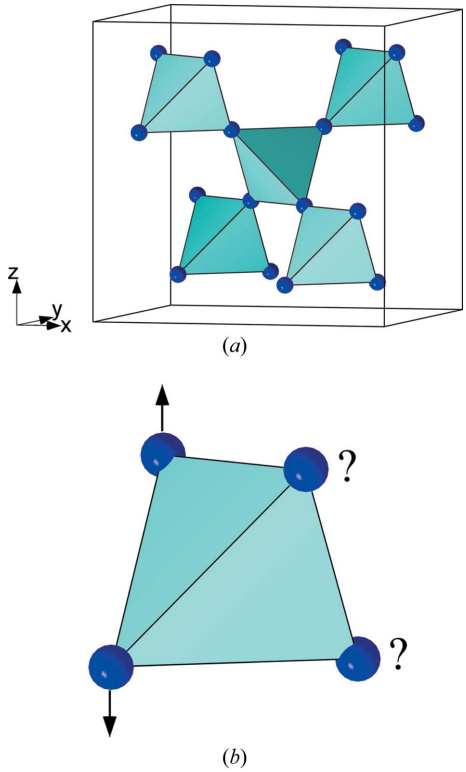

Figure 1
Crystal structure of AB_2O_4 spinel. The *B* ions form the three-dimensional network of corner-sharing tetrahedra (*a*). Spin orientation in the tetrahedron (*b*).

In three dimensions, a frustrated lattice is achieved when spins interact antiferromagnetically in a network of corner-sharing tetrahedra (Bramwell & Gingras, 2001; Moessner & Chalker, 1998). There are three types of structures that can realize a network of corner-sharing tetrahedra: spinels AB_2O_4, pyrochlores $A_2B_2O_7$ and C15 Laves phases AB_2. A great number of chemical substances which crystallize in these structure types are well known.

The ideal cubic spinel is commonly visualized as a three-dimensional network of regular edge-linked BX_6 octahedra, the *B* cations being in the centres of these octahedra, and the *A* cations being centrally located in AX_4 tetrahedra unrelated between themselves. The ideal spinel is cubic with space-group symmetry $Fd\bar{3}m$. The *B* site forms a network of corner-sharing tetrahedra (Fig. 1*a*). The network of these tetrahedra is called a pyrochlore sublattice, for in the pyrochlore structure *B* cations form the same (as in spinels) frustrated sublattice. Spin frustration takes place when on two *B* atoms in the vertices of tetrahedra the spins are located antiferromagnetically, and on the remaining two atoms spins with the same probability can be located both up and down (Fig. 1*b*).

One of the compounds where one can expect unusual physical properties caused by spin frustration is $Na_4Ir_3O_8$ (McDaniel, 1974; Okamoto *et al.*, 2007). Geometrical spin frustration in this compound is due to the existence of an exotic electron structure state of matter which is called spin-liquid (Lawler *et al.*, 2008). The uniqueness of $Na_4Ir_3O_8$ lies in the fact that at ambient pressure it is the first example of a three-dimensional quantum spin-liquid (Okamoto *et al.*, 2007; Podolsky *et al.*, 2009).

One more unique peculiarity is an exotic atomic order which is called 'hyper-kagome order' (Okamoto *et al.*, 2007). Therefore $Na_4Ir_3O_8$ is the object of intense theoretical and experimental research activities (Lawler, Kee *et al.*, 2008; Lawler, Paramekanti *et al.*, 2008; Podolsky *et al.*, 2009; Hopkinson *et al.*, 2007; Chen & Balents, 2008; Zhou *et al.*, 2008; Lee, 2008; Bergholtz *et al.*, 2010; Podolsky & Kim, 2011; Norman & Micklitz, 2010 *etc.*). However, the symmetry and structure aspects of the origin of unique atom hyper-kagome order in $Na_4Ir_3O_8$ require further study. There is also the fundamental problem of whether there are other crystals with hyper-kagome atom order.

There is another motive of the studies described herein: the search for new classes of superconductors and crystals with other abnormal physical properties. This motive is based on an indirect analogy in atom and electron structures of $Na_4Ir_3O_8$ and superconductors. Since Ir is a 5*d* element, the spin–orbit coupling is likely to be much larger than in 3*d* and 4*d* elements. Because of strong spin–orbit coupling, the hyper-kagome lattice is characterized by a half-filled complex of *d* states,

transforming $Na_4Ir_3O_8$ into an analogue of the high-temperature superconducting cuprates (Norman & Micklitz, 2010). It is of interest to note that there is also a strong link between kagome systems with frustration and hole-doped high-T_c cuprate materials. In both cases there is an equivalent degeneracy of ground states but it is due to different mechanisms (Bramwell & Gingras, 2001).

It is also important to note that the space group of the $Na_4Ir_3O_8$ structure, $P4_132$ ($P4_332$), is the same as in the structures of Li_2Pd_3B, Li_2Pt_3B (Eibenstein & Jung, 1997; Lee & Picket, 2005; Bauer & Sigrist, 2012) and Mo_3AlC (Bauer & Sigrist, 2012) superconductors. On doping superconductors with broken mirror symmetry, macroscopic effects are possible which were prohibited in centrosymmetric crystals. One such effect is the magneto-electric effect. Examples of such superconductors are compounds with group symmetry that includes polar axes, such as Mo_3AlC (space group $P4_132$) (Bauer & Sigrist, 2012), LaPtSi (space group $P2_132$) (Bauer & Sigrist, 2012), $La_5B_2C_6$ (space group $P4$) (Bauer & Bars, 1983) and Mo_3P (space group $I\bar{4}2m$) (Sellberg & Rundqvist, 1965).

In this work, based on powerful group-theoretical and advanced thermodynamic methods of Landau phase transition theory (Landau & Lifshitz, 1980; Lifshitz, 1941; Kovalev, 1993; Toledano & Toledano, 1987; Toledano & Dmitriev, 1996; Gufan, 1982) the hyper-kagome order in $Na_4Ir_3O_8$ has been investigated.

By using the concept of one critical irreducible representation (irrep) and the concept of the archetype, the critical order parameter (OP) responsible for the structure $Na_4Ir_3O_8$ formation from the archetype structure has been established. Atom and orbital orderings and structural mechanisms of forming hyper-kagome order in $Na_4Ir_3O_8$ have been studied. Based on the theoretical results obtained and structural experimental data (Okamoto *et al.*, 2007) we have represented the general crystallochemical picture of hyper-kagome order peculiarities in $Na_4Ir_3O_8$. The theoretical analysis has allowed us to predict the existence of new ordered low-symmetry spinel modifications with hyper-kagome order and study the thermodynamic conditions of the origin of hyper-kagome order for a number of cases.

Theoretical methods used in our work have been described in detail in our publications (Sahnenko *et al.*, 1986; Talanov, 1996*a*; Talanov *et al.*, 2013, 2015; Talanov & Shirokov, 2012, 2013*a*,*b*, 2014). We have also checked the separate results obtained by our methods by means of the *ISOTROPY* program (Stokes & Hatch, 2007; Stokes *et al.*, 2002).

2. Atom and orbital order in $Na_4Ir_3O_8$

The substance $Na_4Ir_3O_8$ was mentioned for the first time as an unidentified phase in the Na–Ir–O ternary system by McDaniel (1974). On further investigation it was shown that the substance had a similar structure to $Na_4Sn_3O_8$ (space group $P4_132$ or $P4_332$, $Z = 4$) (Iwasaki *et al.*, 2002). This remarkable material is an insulator with a high Curie–Weiss temperature, $T_W = 650$ K, and a large effective moment, $\mu_{eff} = 1.96$ μB, yet it does not exhibit any sign of magnetic order down to 2 K (Okamoto *et al.*, 2007; Norman & Micklitz, 2010). Space groups $P4_132$ or $P4_332$ and some peculiarities of the $Na_4Ir_3O_8$ structure were established (Okamoto *et al.*, 2007). The Ir and Na ions together occupy the sites of the pyrochlore lattice in such a way that only three of the four sites of each tetrahedron are occupied by Ir (Fig. 2). The lattice of magnetic Ir is a network of corner-sharing triangles as shown in Fig. 2(*a*), where each triangle is derived from different faces of the tetrahedra. In analogy to the kagome lattice in two dimensions, it is called the hyper-kagome lattice (Okamoto *et al.*, 2007).

In a crystal octahedral field formed by oxygen ions, large splitting of energetic levels of Ir^{4+} can be expected. Therefore five *d*-electrons form a low-spin state in the t_{2g} level. Here Ir^{4+} carries spin $S = 1/2$. This gives rise to an antiferromagnetically coupled $S = 1/2$ spin system on a hyper-kagome lattice.

2.1. On the concept of archetype

Many crystalline structures can be considered as pseudo-symmetric with respect to some configuration of higher symmetry. This higher-symmetry arrangement may be another phase of the compound or a virtual reference structure. We will refer to this (real or virtual) structure/phase of higher symmetry as the hypothetical parent structure/phase – the archetype (this word originates from the ancient Greek one $\alpha\rho\chi\varepsilon\tau\upsilon\pi\omega\nu$ which means 'prototype'). The concept of archetype allows us to consider particularities of atom and orbital structure, thermodynamic and substance properties in a unified manner. This concept is widely used in the theory of phase transition (Gufan, 1971; Levanyuk & Sannikov, 1971; Torgashev & Latush, 1997; Dvorak, 1978; Aleksandrov & Beznosikov, 2004). By definition, a group–subgroup relation necessarily exists between the space groups of the archetype structure and the observed one. This latter can then be qualified as a distorted (and/or ordered) structure and can be described as the archetype crystalline structure plus a static symmetry-breaking structural distortion (and/or ordering).

2.2. Archetype of $Na_4Ir_3O_8$

Our analysis is based on the hypothesis that the $Na_4Ir_3O_8$ archetype is a spinel-like structure with space group $Fd\bar{3}m$ and it has the composition $[Na_{1/2}Ir_{3/2}]^{16d}[Na_{3/2}]^{16c}O^{32e}{}_4$. To confirm this hypothesis, we present three arguments: (i) crystallochemical closeness of the archetype structure and the $Na_4Ir_3O_8$ structure; (ii) the space group of the $Na_4Ir_3O_8$ structure is a subgroup of the symmetry group of the archetype structure; (iii) the multiplication of primitive cell volume as a result of a hypothetical phase transition from the high-symmetry archetype to the cubic $Na_4Ir_3O_8$ structure is exactly equal to the multiplication of the primitive cell volume for the proposed OP. These arguments will be considered in detail.

In the opinion of Okamoto *et al.* (2007), the $Na_4Ir_3O_8$ structure is close to a cubic spinel structure (space group $Fd\bar{3}m$). In this case one can suppose that the structure formula of $Na_4Ir_3O_8$ should be given by $(Na_{3/2})_1[Ir_{3/4}Na_{1/4}]_2O_4$. Then it is similar to the structure formula of spinel, $(A)^{8a}[B]^{16d}{}_2O^{32e}{}_4$.

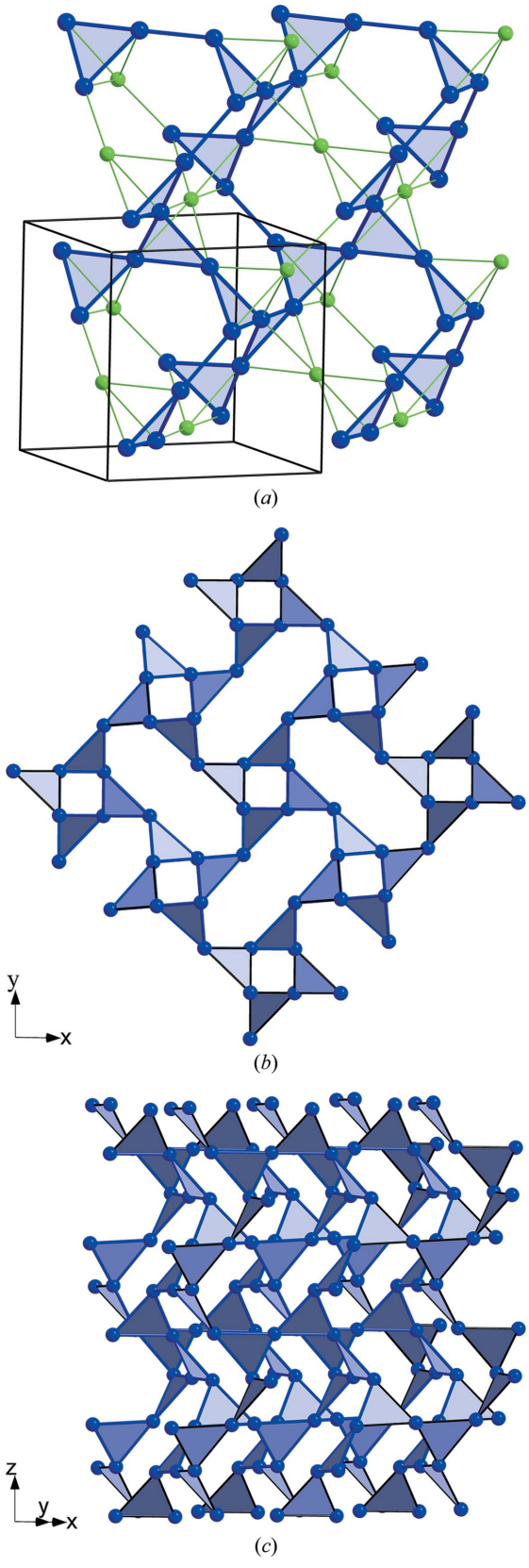

Figure 2
A hyper-kagome sublattice. A hyper-kagome sublattice is a cubic lattice with 12 sites in a unit cell; it is a network of corner-sharing Ir triangles (*a*). View of the hyper-kagome sublattice along the direction [001] (*b*); general picture (*c*).

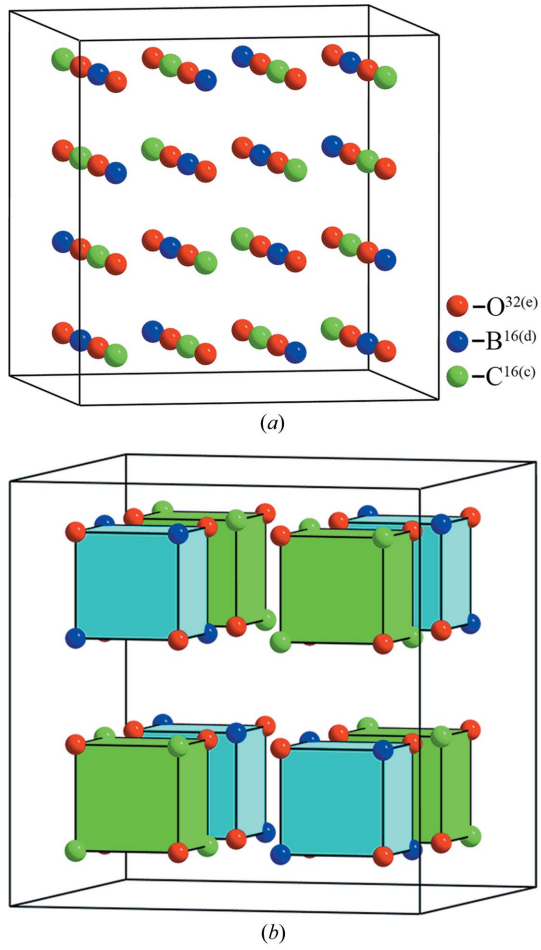

Figure 3
Hypothetical structure with composition $[B_2]^{16d}[C_{3/2}]^{16c}O^{32e}{}_4$. Atom representation of structure (*a*), hexahedral representation (*b*). Wyckoff position 16*d* is occupied by Ir (75%) and Na (25%) atoms.

In this formula there are atoms occupying Wyckoff position 8*a* in parentheses and there are atoms occupying Wyckoff position 16*d* in square brackets (Okamoto *et al.*, 2007). However, we note the fundamental differences between the spinel structure and the $Na_4Ir_3O_8$ structure: (i) in the spinel structure in one formula unit there is one but not 3/2 tetrahedral atoms; (ii) an excessive number of Na atoms leads to the fact that the tetrahedral atoms in the considered structure will occupy not one but several Wyckoff positions.

Okamoto *et al.* (2007) believe that the Na atoms in the $Na_4Ir_3O_8$ structure occupy octahedral positions but not tetrahedral 8*a* Wyckoff positions in spinel structure. We consider that the $Na_4Ir_3O_8$ archetype is not a spinel structure but a spinel-like structure with $[Na_{1/2}Ir_{3/2}]^{16d}[Na_{3/2}]^{16c}O^{32e}{}_4$ composition [space group $Fd\bar{3}m$ (Z_P = 2, Z_B = 8)] (Fig. 3). Hereafter Z_P is the number of formula units in the primitive cell while Z_B is the same in the Bravais cell. In the primitive cell of the spinel-like structure of $Na_4Ir_3O_8$ there are 15 atoms but in the primitive cell of the $Na_4Ir_3O_8$ archetype structure there are 60 atoms. The number of formula units in the primitive cell of the observed phase determines the type of reduction of the translational symmetry and the Bravais lattice

of the archetype structure. The transformation properties of the OP with respect to the translation operation restrict the ratio of the number of formula units in the primitive cell of the low-symmetry phase to the number of formula units in the high-symmetry phase (*i.e.* the number of formula units in the archetype structure). This conclusion comes from the results of the work by Lifshitz (1941). In this work it is established how many times the volume of the primitive cell increases as a result of phase transition if the vector **k**, to which the critical irrep belongs and according to which the OP is transformed, occupies a special position in the reciprocal lattice of a high-symmetry phase.

The archetype structure proposed by the authors is significantly different from spinel structure: (i) Wyckoff position 8*a* in the archetype structure is vacant; (ii) Wyckoff position 16*c* in spinel structure is vacant, and in the archetype structure (as in the $Na_4Ir_3O_8$ structure) this position is occupied by 75% Na^{1+} ions.

Therefore the archetype does not possess a spinel structure, but has a spinel-like structure.

Among spinel-like structures there are no stable substances that have an atom distribution on Wyckoff positions strictly corresponding to the structure formula $[B_2]^{16d}[C_{3/2}]^{16c}O^{32e}{}_4$. Therefore, the archetype structure is a hypothetical structure. But structures are known that have the $Fd\bar{3}m$ space group and that are close to the structure of $[Na_{1/2}Ir_{3/2}]^{16d}$-$[Na_{3/2}]^{16c}O^{32e}{}_4$. For example, carbides $Ti_{0.8}V_{0.2}C_{0.62}$ are characterized by a distribution of cations $[C2_{0.53}]^{16d}{}_2$-$[C1_{0.71}]^{16c}{}_2[Ti_{0.8}V_{0.2}]^{32e}{}_4$ (Tashmetov *et al.*, 2005). Metastable spinel-like modification of λ-MnO_2 has a rutile structure (Greedan *et al.*, 1998). λ-MnO_2 is formed as a result of electrochemical Li deintercalation from $LiMn_2O_4$ cathodes in solid-state lithium batteries during charge/discharge cycling. Ions of Mn^{4+} in λ-MnO_2 occupy Wyckoff position 16*d*. They form a three-dimensional framework from tetrahedra connected by corners. Oxygen ions occupy Wyckoff position 32*e*, and Wyckoff positions 8*a* and 16*c* are vacant. λ-MnO_2 has the same structure as that of Ir_2O_4. Ir_2O_4 is epitaxically stabilized iridium spinel oxide without cations in the tetrahedral sites, which is composed of an Ir^{4+} pyrochlore lattice (Kuriyama *et al.*, 2010). The λ-MnO_2-type of Ir_2O_4 is obtained by employing a thin-film technique and a soft chemical method (Kuriyama *et al.*, 2010). A spinel oxide with Ir has not been synthesized yet in the bulk form. The only known spinel-type Ir oxides is $ZnIr_2O_4$, which was stabilized by utilizing a thin-film technique (Dekkers *et al.*, 2007).

2.3. OP symmetry of a hypothetical phase transition

The structure of the low-symmetry cubic $Na_4Ir_3O_8$ phase is organically connected with the archetype structure by atom displacements and their ordering, *i.e.* by a hypothetical phase transition. In order to derive the $Na_4Ir_3O_8$ structure theoretically from the archetype structure it is necessary to establish a critical order parameter, inducing this hypothetical phase transition.

First of all we note that space groups $P4_132$ and $P4_332$ are subgroups of space groups $Pm\bar{3}n$ (8), $Pn\bar{3}m$ (8), $Fm\bar{3}m$ (32), $Fd\bar{3}m$ (4), $Fd\bar{3}c$ (4), $Ia\bar{3}d$ (2), $P4_232$ (4), $F432$ (32), $F4_132$ (4) and $I4_132$ (2). The multiplication in the primitive cell volumes as a result of phase transitions from phases of the given symmetry to $P4_132$ or $P4_332$ phases is shown in parentheses.

As a result of a hypothetical phase transition to $P4_132$ or $P4_332$ phases the primitive cell volume increases by four times. This means that space groups of the archetype structure can only be the groups $Fd\bar{3}m$ (4), $Fd\bar{3}c$ (4) and $F4_132$ (4). Taking into consideration the crystallochemical closeness of the $Na_4Ir_3O_8$ structure and the spinel-like archetype of composition $[Na_{1/2}Ir_{3/2}]^{16d}[Na_{3/2}]^{16c}O^{32e}{}_4$, it follows that the critical irrep τ, generating the appearance of the $P4_132$ ($P4_332$) phase from a high-symmetry spinel-like phase with space group $Fd\bar{3}m$, is the six-dimensional irrep $\boldsymbol{\kappa}_{10}(\tau_1)$ [the indexing of vectors and irreps is given according to Kovalev (1993)]. The correspondence of the designation by Kovalev and Miller & Love (which is used in the program *ISOTROPY*) is as follows: $\mathbf{k}_{10}(X)$: $\tau_1 - X3$ (Stokes & Hatch, 2007).

Table 1 lists the space groups of all possible low-symmetry phases induced by irrep $\boldsymbol{\kappa}_{10}(\tau_1)$, and corresponding components of the six-dimensional OP. As well as the multiplication of primitive cell volumes as a result of the structural phase transitions (V_0/V), the vectors of primitive cell translations of low-symmetry phases ($\mathbf{a}_1$, $\mathbf{a}_2$, $\mathbf{a}_3$) and the structure formulas of low-symmetry phases are presented.

Among these low-symmetry phases there is a phase with the $Na_4Ir_3O_8$ structure. The direction in six-dimensional space of OP $(0, \varphi, 0, \varphi, 0, -\varphi)$ and space group $P4_132$ correspond to this phase. The direction in space of OP $(0, \varphi, 0, \varphi, 0, -\varphi, 0)$ and space group $P4_332$ correspond to another enantiomorphic structure of $Na_4Ir_3O_8$. An enantiomorphic structure is a spatial distribution of charge or spin density that does not coincide with its mirror image after any combination of rotations and translations. These mirror modifications are different domains of the $Na_4Ir_3O_8$ structure. Previously it was experimentally established that enantiomorphic modifications of low-symmetry spinel phases were observed on one sample as different domains (Van der Biest & Thomas, 1975).

2.4. Structure mechanism of the formation of atom hyper-kagome order in $Na_4Ir_3O_8$

As a result of a hypothetical phase transition from the archetype structure, Wyckoff-position splitting takes place. Wyckoff position 16*d* in the archetype structure splits into Wyckoff positions 4*b* and 12*d* in the $P4_132$ ($P4_332$) structure, Wyckoff position 16*c* splits into Wyckoff positions 4*a* and 12*d*, and Wyckoff position 32*e* splits into Wyckoff positions 8*c* and 24*e*. Taking into account the occupancy of Wyckoff position 16*c* by 75% (Okamoto *et al.*, 2007), the structure formula $Na_4Ir_3O_8$ in $P4_132$ ($P4_332$) phases can be written as $[Na^{4b}{}_{1/2}Ir^{12d}{}_{3/2}][Na^{4a}{}_{3/8}Na^{12d}{}_{9/8}]O^{8c}O^{24e}{}_3$. Note that in investigating the $Na_4Sn_3O_8$ structure, which has the same structure as $Na_4Ir_3O_8$, Iwasaki *et al.* (2002) admitted the possibility that the site occupied partially by the sodium ion is divided into two or

Table 1
Low-symmetry crystal phases generated by irrep $\mathbf{k}_{10}(\tau_1)$ of space group $Fd\bar{3}m$.

The superscript index in the structural formula means the type of Wyckoff position according to *International Tables for Crystallography*. The superscript on the brackets is the repetition number of the position.

φ	Symbol of space group	Translations of primitive cell of spinel structure	V_0/V	Structural formula
$(0, \varphi, 0, \varphi, 0, -\varphi)$ $(\varphi, 0, \varphi, 0, -\varphi, 0)$	$P4_132$ (No. 213) $P4_332$ (No. 212)	$\mathbf{a}_1+\mathbf{a}_2+\mathbf{a}_3$, $2\mathbf{a}_2$, $2\mathbf{a}_1$	4	$A^c{}_{16}B^a{}_8B^d{}_{24}X^c{}_{16}X^e{}_{48}C^b{}_8C^d{}_{24}$
$(\varphi, \varphi, \varphi, \varphi, \varphi, \varphi)$	$R\bar{3}m$ (No. 166)	$\mathbf{a}_1+\mathbf{a}_2+\mathbf{a}_3$, $2\mathbf{a}_2$, $2\mathbf{a}_1$	4	$A^c{}_4A^h{}_{12}B^b{}_2B^d{}_6B^h{}_{12}B^f{}_{12}X^c{}_4(X^h{}_{12})^3X^i{}_{24}C^a{}_2C^e{}_6C^h{}_{12}C^g{}_{12}$
$(0, 0, 0, 0, 0, \varphi)$ $(0, 0, 0, 0, \varphi, 0)$	$P4_122$ (No. 91) $P4_322$ (No. 95)	$\mathbf{a}_1+\mathbf{a}_3$, $\mathbf{a}_1$, $2\mathbf{a}_1$	2	$A^c{}_{16}B^a{}_{16}B^b{}_{16}(X^d{}_{32})^2C^a{}_{16}C^b{}_{16}$
$(0, \varphi, 0, 0, \varphi, 0)$	$P\bar{4}2_1m$ (No. 113)	$\mathbf{a}_1+\mathbf{a}_2+\mathbf{a}_3$, $2\mathbf{a}_2$, $2\mathbf{a}_1$	4	$A^b{}_4A^c{}_4A^e{}_8(B^e{}_8)^2B^f{}_{16}(X^e{}_8)^4(X^f{}_{16})^2(C^e{}_8)^2C^f{}_{16}$
$(0, 0, \varphi, \varphi, 0, 0)$	$Pbmn$ (No. 53)	$\mathbf{a}_2+\mathbf{a}_3$, $2\mathbf{a}_2$, $\mathbf{a}_1$	2	$A^h{}_{16}B^b{}_8B^c{}_8B^g{}_{16}(X^h{}_{16})^2X^i{}_{32}C^a{}_8C^d{}_8C^g{}_{16}$
$(\varphi_1, \varphi_2, \varphi_1, \varphi_2, \varphi_1, \varphi_2)$	$R32$ (No. 155)	$\mathbf{a}_1+\mathbf{a}_2+\mathbf{a}_3$, $2\mathbf{a}_2$, $2\mathbf{a}_1$	4	$A^c{}_4A^f{}_{12}B^b{}_2B^e{}_6(B^d{}_6)^2B^f{}_{12}X^c{}_4(X^f{}_{12})^5C^a{}_2(C^e{}_6)^2C^d{}_6C^f{}_{12}$
$(\varphi_1, 0, 0, \varphi_2, 0, 0)$	$P2_12_12$ (No. 18)	$\mathbf{a}_1+\mathbf{a}_2+\mathbf{a}_3$, $2\mathbf{a}_2$, $2\mathbf{a}_1$	4	$A^a{}_4A^b{}_4A^c{}_8(B^c{}_8)^4(X^c{}_8)^8(C^c{}_{88})^4$
$(0, 0, 0, 0, \varphi_1, \varphi_2)$	$P222_1$ (No. 17)	$\mathbf{a}_2+\mathbf{a}_3$, $2\mathbf{a}_2$, $\mathbf{a}_1$	2	$A^e{}_{16}B^a{}_8B^b{}_8B^c{}_8B^d{}_8(X^e{}_{16})^4C^a{}_8C^b{}_8C^c{}_8C^d{}_8$
$(0, \varphi_1, 0, \varphi_2, 0, -\varphi_1)$ $(\varphi_1, 0, \varphi_2, 0, -\varphi_1, 0)$	$P4_12_12$ (No. 92) $P4_32_12$ (No. 96)	$\mathbf{a}_1+\mathbf{a}_2+\mathbf{a}_3$, $2\mathbf{a}_2$, $2\mathbf{a}_1$	4	$A^b{}_{16}(B^a{}_8)^2B^b{}_{16}(X^b{}_{16})^4(C^a{}_8)^2C^b{}_{16}$
$(\varphi_1, \varphi_1, \varphi_2, \varphi_2, -\varphi_1, -\varphi_1)$	$C2/m$ (No. 12)	$\mathbf{a}_1+\mathbf{a}_2+\mathbf{a}_3$, $2\mathbf{a}_2$, $2\mathbf{a}_1$	4	$(A^i{}_4)^2A^j{}_8B^c{}_2B^d{}_2B^e{}_4B^g{}_4B^i{}_4(B^j{}_8)^2(X^i{}_4)^4(X^j{}_8)^6C^a{}_2C^b{}_2$-$C^f{}_4C^h{}_4(C^j{}_8)^2$
$(\varphi_1, 0, \varphi_2, 0, \varphi_3, 0)$	$P2_12_12_1$ (No. 19)	$\mathbf{a}_1+\mathbf{a}_2+\mathbf{a}_3$, $2\mathbf{a}_2$, $2\mathbf{a}_1$	4	$(A^a{}_8)^2(B^a{}_8)^4(X^a{}_8)^8(C^a{}_8)^4$
$(\varphi_1, 0, \varphi_2, \varphi_3, -\varphi_1, 0)$	$C222_1$ (No. 20)	$\mathbf{a}_1+\mathbf{a}_2+\mathbf{a}_3$, $2\mathbf{a}_2$, $2\mathbf{a}_1$	4	$(A^c{}_8)^2(B^a{}_4)^2(B^b{}_4)^2(B^c{}_8)^2(X^c{}_8)^8(C^a{}_4)^2(C^b{}_4)^2(C^c{}_8)^2$
$(\varphi_1, \varphi_1, \varphi_2, \varphi_2, \varphi_3, \varphi_3)$	$P\bar{1}$ (N2)	$\mathbf{a}_1+\mathbf{a}_2+\mathbf{a}_3$, $2\mathbf{a}_2$, $2\mathbf{a}_1$	4	$(A^i{}_4)^4B^b{}_2B^c{}_2B^d{}_2B^h{}_2(B^i{}_4)^6(X^i{}_4)^{16}C^a{}_2C^e{}_2C^f{}_2C^g{}_2(C^i{}_4)^6$
$(\varphi_1, \varphi_1, \varphi_2, \varphi_3, \varphi_3, \varphi_2)$	Cm (No. 8)	$\mathbf{a}_1+\mathbf{a}_2+\mathbf{a}_3$, $2\mathbf{a}_2$, $2\mathbf{a}_1$	4	$(A^a{}_2)^4(A^b{}_4)^2(B^a{}_2)^4(B^b{}_4)^6(X^a{}_2)^8(X^b{}_4)^{12}(C^a{}_2)^4(C^b{}_4)^6$
$(\varphi_1, \varphi_2, \varphi_3, \varphi_4, \varphi_3, \varphi_4)$	$C2$ (No. 5)	$\mathbf{a}_1+\mathbf{a}_2+\mathbf{a}_3$, $2\mathbf{a}_2$, $2\mathbf{a}_1$	4	$(A^c{}_4)^4(B^a{}_2)^2(B^b{}_2)^2(B^c{}_4)^6(X^c{}_4)^{16}(C^a{}_2)^2(C^b{}_2)^2(C^c{}_4)^6$
$(0, \varphi_1, 0, \varphi_2, \varphi_3, \varphi_4)$	$P2_1$ (No. 4)	$\mathbf{a}_1+\mathbf{a}_2+\mathbf{a}_3$, $2\mathbf{a}_2$, $2\mathbf{a}_1$	4	$(A^a{}_4)^4(B^a{}_4)^8(X^a{}_4)^{16}(C^a{}_4)^8$
$(\varphi_1, \varphi_2, \varphi_3, \varphi_4, \varphi_5, \varphi_6)$	$P1$ (No. 1)	$\mathbf{a}_1+\mathbf{a}_2+\mathbf{a}_3$, $2\mathbf{a}_2$, $2\mathbf{a}_1$	4	$(A^a{}_4)^8(B^a{}_2)^{16}(X^a)^{32}(C^a{}_2)^{16}$

more crystallographic sites. Our theoretical results show that no further splitting of Wyckoff positions either for iridium or for sodium should exist.

Note that, from the structure formula, it follows that in compound $Na_4Ir_3O_8$ there cannot be, in principle, a charge ordering of iridium atoms as iridium atoms occupy only one Wyckoff position 12*d* with local symmetry 2 (C_2) (Table 1).

To establish the structure mechanism of forming unique hyper-kagome order in the $Na_4Ir_3O_8$ structure, it is necessary to analyse the entry of critical irrep $\boldsymbol{\kappa}_{10}(\tau_1)$ into mechanical, permutation and orbital representations of the spinel-like structure of $[B_2]^{16d}[C_{3/2}]^{16c}O^{32e}{}_4$. For this structure, the first Brillouin zone represents a body-centred lattice and contains four points of high symmetry, namely: $\mathbf{k}_{11}(\Gamma)$, $\mathbf{k}_{10}(X)$, $\mathbf{k}_9(L)$ and $\mathbf{k}_8(W)$ (Kovalev, 1993). For these points there are stars of the following wavevectors: $\mathbf{k}_{11} = 0$; $\mathbf{k}_{10} = 1/2(b_1 + b_2)$; $\mathbf{k}_9 = 1/2(b_1 + b_2 + b_3)$; $\mathbf{k}_8 = b_1/4 - b_2/4 + b_3/2$. The indexing of vectors and irreps is given according to Kovalev (1993). The composition of the mechanical and permutation representations for Wyckoff positions 16*d*, 16*c* and 32*e* of the space group $Fd\bar{3}m$ are partially given in Sahnenko *et al.* (1986), Talanov *et al.* (2013, 2015) and Talanov & Shirokov (2012, 2014).

The composition of the mechanical representation of crystals (τ_M) with the hypothetical spinel-like structure is as follows.

Wyckoff position 16*d*:

$$\tau_M = \mathbf{k}_{11}(\tau_4 + \tau_6 + \tau_8 + 2\tau_{10}) + \mathbf{k}_{10}(\tau_1 + 2\tau_2 + 2\tau_3 + \tau_4) + \mathbf{k}_9(\tau_1 + \tau_2 + 2\tau_4 + \tau_5 + 3\tau_6). \quad (1)$$

Wyckoff position 16*c*:

$$\tau_M = \mathbf{k}_{11}(\tau_4 + \tau_6 + \tau_8 + 2\tau_{10}) + \mathbf{k}_{10}(\tau_1 + 2\tau_2 + 2\tau_3 + \tau_4) + \mathbf{k}_9(2\tau_1 + \tau_2 + \tau_4 + 3\tau_5 + \tau_6). \quad (2)$$

Wyckoff position 32*e*:

$$\tau_M = \mathbf{k}_{11}(\tau_1 + \tau_4 + \tau_5 + \tau_6 + 2\tau_7 + \tau_8 + \tau_9 + 2\tau_{10}) + \mathbf{k}_{10}(3\tau_1 + 3\tau_2 + 4\tau_3 + 2\tau_4) + \mathbf{k}_9(3\tau_1 + \tau_2 + \tau_3 + 3\tau_4 + 4\tau_5 + 4\tau_6). \quad (3)$$

The composition of the permutation representation of crystals (τ_p) with the hypothetical spinel-like structure is as follows.

Wyckoff position 16*d*:

$$\tau_p = \mathbf{k}_{11}(\tau_1 + \tau_7) + \mathbf{k}_{10}(\tau_1 + \tau_3) + \mathbf{k}_9(\tau_1 + \tau_4 + \tau_5). \quad (4)$$

Wyckoff position 16*c*:

$$\tau_p = \mathbf{k}_{11}(\tau_1 + \tau_7) + \mathbf{k}_{10}(\tau_1 + \tau_3) + \mathbf{k}_9(\tau_1 + \tau_4 + \tau_6). \quad (5)$$

Wyckoff position 32*e*:

$$\tau_p = \mathbf{k}_{11}(\tau_1 + \tau_4 + \tau_7 + \tau_{10}) + \mathbf{k}_{10}(\tau_1 + \tau_2 + 2\tau_3) + \mathbf{k}_9(2\tau_1 + 2\tau_4 + \tau_5 + \tau_6). \quad (6)$$

Analysis of expressions (1)–(6) shows that the $Na_4Ir_3O_8$ structure is formed from a spinel-like archetype structure with composition $[Na_{1/2}Ir_{3/2}]^{16d}[Na_{3/2}]^{16c}O^{32e}{}_4$ as a result of displacements of Na, Ir and O atoms and also as a result of ordering Na, Ir and O atoms. We have built the scalar and vector basic functions of irrep $\mathbf{k}_{10}(\tau_1)$ which allowed us to calculate the $Na_4Ir_3O_8$ atom structure. The results of theoretical calculations of the $Na_4Ir_3O_8$ atom structure are given below.

2.5. Crystallochemistry of $Na_4Ir_3O_8$

The structure of $Na_4Ir_3O_8$ can be theoretically derived from the archetype phase having composition $[Na_{1/2}Ir_{3/2}]^{16d}$-$[Na_{3/2}]^{16c}O^{32e}{}_4$ and spinel-like structure as a result of displacements and ordering (type 1:3) of all atoms (Fig. 4).

All ions in the $Na_4Ir_3O_8$ structure are in the centres of distorted octahedra. There are several types of distorted octahedra. Na^{4a} and Na^{4b} ions are in the centres of monoclinically distorted octahedra $[Na^{4a}O^{24e}{}_6]$ and $[Na^{4b}O^{24e}{}_6]$ formed by six ions of oxygen O^{24e}. Na^{12d} ions are in the centres of trigonally distorted octahedra $[Na^{12d}O^{24e}{}_4O^{8c}{}_2]$ formed by four ions of oxygen O^{24e} and by two ions of oxygen O^{8c}. Distorted IrO_6 octahedra $[IrO^{24e}{}_4O^{8c}{}_2]$ are formed by four ions of oxygen O^{24e} and by two ions of oxygen O^{8c}. Each oxygen ion O^{8c} is in the centre of trigonally distorted octahedra $[O^{8c}Ir^{12d}{}_3Na^{12d}{}_3]$ and each oxygen ion O^{24e} is in the centre of triclinically distorted octahedra $[O^{24e}Ir^{12d}{}_2Na^{12d}{}_2$-$Na^{4a}Na^{4b}]$.

Enantiomorphic forms of $Na_4Ir_3O_8$ are mirror antipodes. Their structures coincide with each other only by reflection in a mirror (Fig. 5). The chemical and physical properties of the enantiomorphic modifications of $Na_4Ir_3O_8$ are the same (except optical activity).

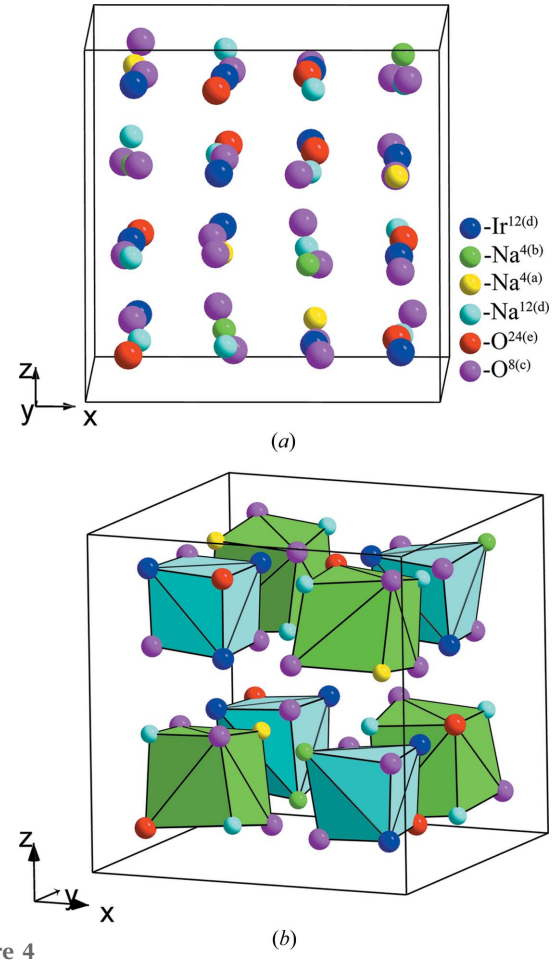

Figure 4
$Na_4Ir_3O_8$ structure: atom representation (*a*), hexahedral representation (*b*).

It is interesting to note that the structure $Na_4Ir_3O_8$ may be represented by a network of double helices. One helix is formed by distorted hexahedra $[Ir^{12d}{}_3Na^{4b}O^{24e}{}_3O^{8c}]$ and the other helix is formed by distorted hexahedra $[Na^{4a}Na^{12d}{}_3O^{24e}{}_3O^{8c}]$ (Fig. 6*a*).

This double helix is topologically similar to the double helix of the DNA molecule. Among inorganic and organic crystals, substances are found with structures that can be represented by double helices (Talanov, 1996*b*, 2007; Talanov *et al.*, 2008; Talanov & Ereyskaya, 2014; Gieck *et al.*, 2004; Bostrom & Lidin, 2002; Jeanneau *et al.*, 2002; Zhu *et al.*, 2010). There are, of course, fundamental differences between the structures of inorganic and biochemical compounds containing double helices. The main difference is the fact that the DNA molecule is autonomous, while in inorganic crystals double helices are not independent structure units: they are interconnected. In this case a crystal is the network of helices coupled to each other (Fig. 6*b*).

Metal atoms in the $Na_4Ir_3O_8$ structure form two different networks of tetrahedra: $[Na^{12d}{}_3Na^{4a}]$ and $[Ir^{12d}{}_3Na^{4b}]$ (Fig. 7). Each of these networks forms its own hyper-kagome sublattice. A hyper-kagome sublattice in a network of tetrahedra $[Na^{12d}{}_3Na^{4a}]$ is formed by triangles $[Na^{12d}{}_3]_n$. This hyper-kagome sublattice has artificial character from the point of view of physics because there is no principal difference in the properties of Na^{12d} and Na^{4a} ions.

The $[Ir^{12d}{}_3]_n$ hyper-kagome sublattice in the $Na_4Ir_3O_8$ structure has significant physical importance. In this hyper-kagome sublattice in each tetrahedron three vertices are occupied by magnetic ions Ir^{12d} and one vertex is occupied by sodium ion Na^{4b} (Fig. 2*a*). Four tetrahedra form a hyper-tetrahedron $[Ir^{12d}{}_3Na^{4b}]_4$. From the network of hyper-tetrahedra $[Ir^{12d}{}_3Na^{4b}]_4$ the hyper-kagome sublattice is formed in the following way. In each tetrahedron a regular triangle $[Ir^{12d}{}_3]$ is formed from Ir atoms. All positions of Ir ions in the $Na_4Ir_3O_8$ structure are equivalent, all Ir—Ir distances are the same and are 3.112 Å (Giauque & Stout, 1936). These regular triangles form a network $[Ir^{12d}{}_3]_n$ from *n* triangles $[Ir^{12d}{}_3]$. This network of connected triangles forms unique atom hyper-kagome order (Okamoto *et al.*, 2007) (Figs. 2*b*,*c*).

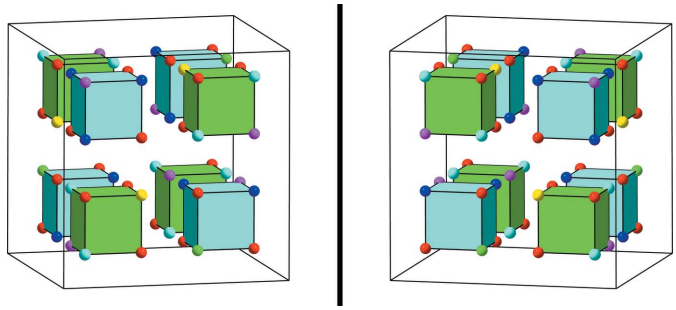

Figure 5
Ordered distribution of cations and anions in enantiomorphic structures, $P4_332$ and $P4_132$ modifications of $Na_4Ir_3O_8$. Hexahedra are shown without taking into account atom displacements. The line between the structures denotes a mirror. The designation of atom types by colour is the same as in Fig. 4(*a*).

In the hyper-kagome sublattice $[Ir^{12d}{}_3]_n$ it is possible to specify a module from three crossing minimal closed contours (loops) of Ir—Ir bonds (Fig. 8). This module consists of 14 iridium triangles. Two of these triangles are common for all three minimal contours. The perimeter of all minimal contours is the same and equal to 31.12 Å. The shortest contour includes ten Ir—Ir bonds. This contour is called a 'decagon' (Bergholtz *et al.*, 2010) (Fig. 9). The longest distance between opposite Ir atoms in a decagon is 10.775 Å and the maximum width of a decagon is 5.659 Å.

It is interesting to note the structure similarity of $[Ir^{12d}{}_3Na^{4b}]_4$ clusters and discrete Rh_4 tetrahedra in superconductors in ternary lanthanide rhodium borides: $LnRh_4B_4$ (Ln, certain lanthanides such as Nd, Sm, Er, Tm, Lu) (King,

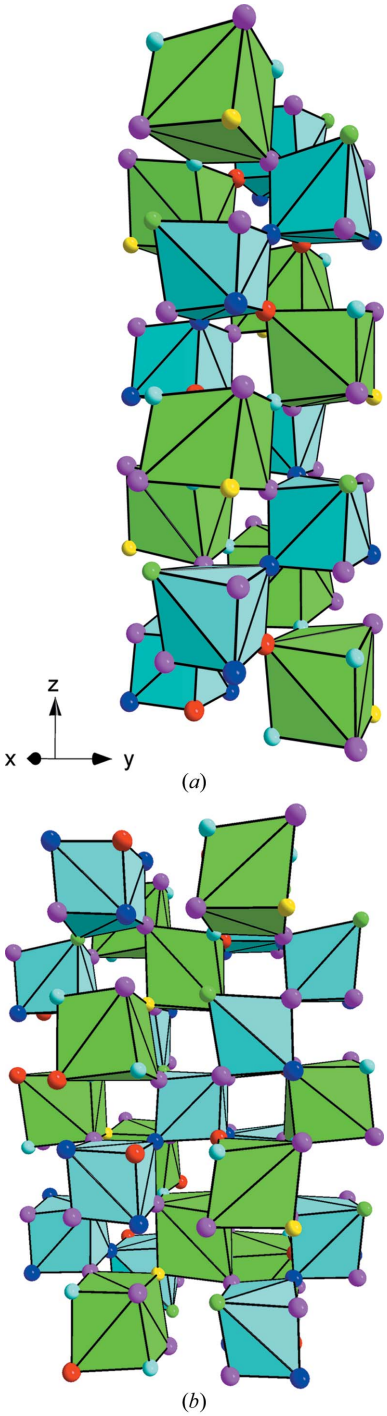

Figure 6
Double helix formed from distorted hexahedra $[Ir^{12d}{}_3Na^{4b}O^{24e}{}_3O^{8c}]$ (dark blue) and $[Na^{4a}Na^{12d}{}_3O^{24e}{}_3O^{8c}]$ (green) (*a*), two double helices in the $Na_4Ir_3O_8$ structure (*b*).

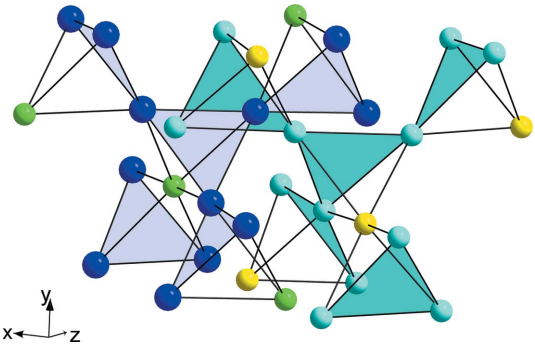

Figure 7
Two networks of tetrahedra $[Na^{12d}{}_3Na^{4a}]$ and $[Ir^{12d}{}_3Na^{4b}]$ forming two hyper-kagome sublattices.

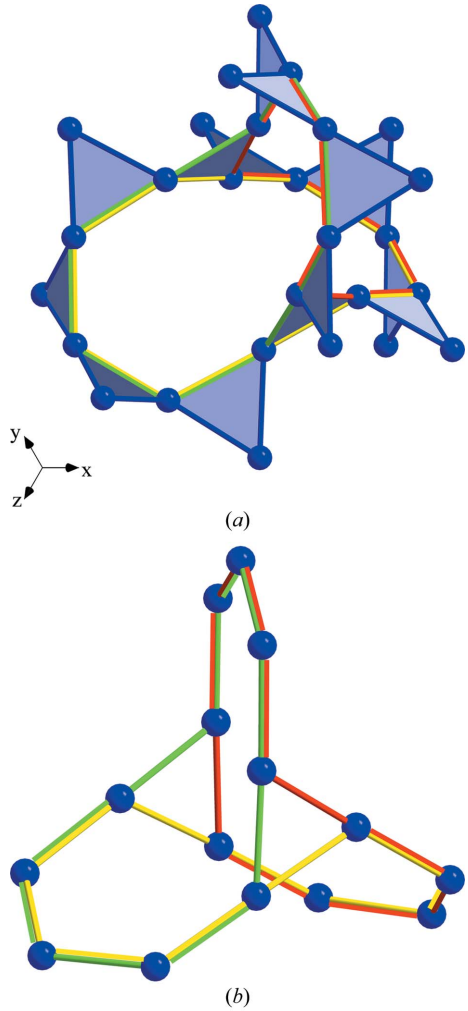

Figure 8
Structure module of $Na_4Ir_3O_8$, consisting of three contours. Contours consist of triangles $[Ir^{12d}{}_3]$ (*a*), three minimal intercrossing contours of Ir—Ir bonds (*b*). Each contour is designated by one colour.

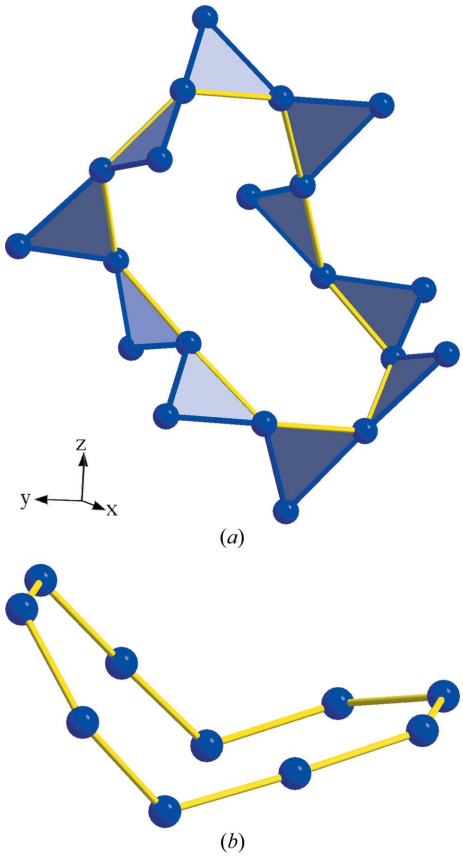

Figure 9
Decagons in $Na_4Ir_3O_8$ structure. Contour from ten triangles [$Ir^{12d}{}_3$] (*a*), the decagon is the minimal closed contour from Ir atoms (*b*).

1987). These rhodium borides have a structure consisting of electronically linked Rh_4 tetrahedra. A similar bond, formed as a result of d_{xy}, d_{xz}, d_{yz} orbital ordering of Rh in $LnRh_4B_4$, also exists in the $Na_4Ir_3O_8$ hyper-kagome sublattice.

2.6. Orbital structure of the $[Ir^{12d}{}_3]_n$ hyper-kagome sublattice

For investigating the ordering of the d_{xy}, d_{xz}, d_{yz} orbitals in the $Na_4Ir_3O_8$ structure, an orbital representation should be built. The orbital representation is built like the mechanical one, only instead of matrices of atom displacements, matrices of transformations of *d* orbitals are used. In the case of spherical symmetry of hydrogen-like atoms, wavefunctions of *d* orbitals are converted according to a five-dimensional irrep of $O(3)^+$ group symmetry and correspond to the square of the vector representation, except the unit irrep. By lowering the symmetry to cubic, the five-dimensional representation of *d* orbitals splits into two irreps: three-dimensional F_{2g}, according to which d_{xy}, d_{xz}, d_{yz} orbitals are transformed, and two-dimensional E_g which are built on the linear combinations of d_{xx}, d_{yy}, d_{zz} orbitals.

Ir^{4+} ions are located in Wyckoff position 16*d* of the spinel-like archetype structure. The composition of the orbital representation on this position obtained on d_{xy}, d_{xz}, d_{yz} orbital ordering is as follows (Talanov *et al.*, 2013, 2015):

$$\tau = \mathbf{k}_{11}(\tau_1 + \tau_5 + 2\tau_7 + \tau_9) + \mathbf{k}_{10}(2\tau_1 + \tau_2 + 2\tau_3 + \tau_4) + \mathbf{k}_9(2\tau_1 + \tau_3 + \tau_4 + 3\tau_5 + \tau_6). \quad (7)$$

Irrep $\mathbf{k}_{10}(\tau_1)$ enters into the composition of the orbital representation. It means that formation of the hyper-kagome sublattice in the structure of $Na_4Ir_3O_8$ is accompanied by ordering d_{xy}, d_{xz}, d_{yz} orbitals. An additional factor which was taken into account in group-theoretical calculations is the sign of the wavefunction. This factor is sufficient for orbitals not possessing spherical symmetry (Fig. 10).

The signs of the 'petals' of the wavefunctions that lie on opposite sides of the nodal plane are opposite. The existence of signs obtained as a result of application of symmetry operations to the *d* orbitals is connected with the presence of signs of the 'petals' of the wavefunctions (Fig. 10). The orbital structure of $Na_4Ir_3O_8$ appears to be very complex even in the absence of spin–orbit interaction and other physical effects. Therefore further mutual group-theoretical and model microscopical analysis is required.

The pictures of *d*-orbital ordering, the structure mechanism of hyper-kagome sublattice formation and features of crystallochemistry can become the basis for the construction

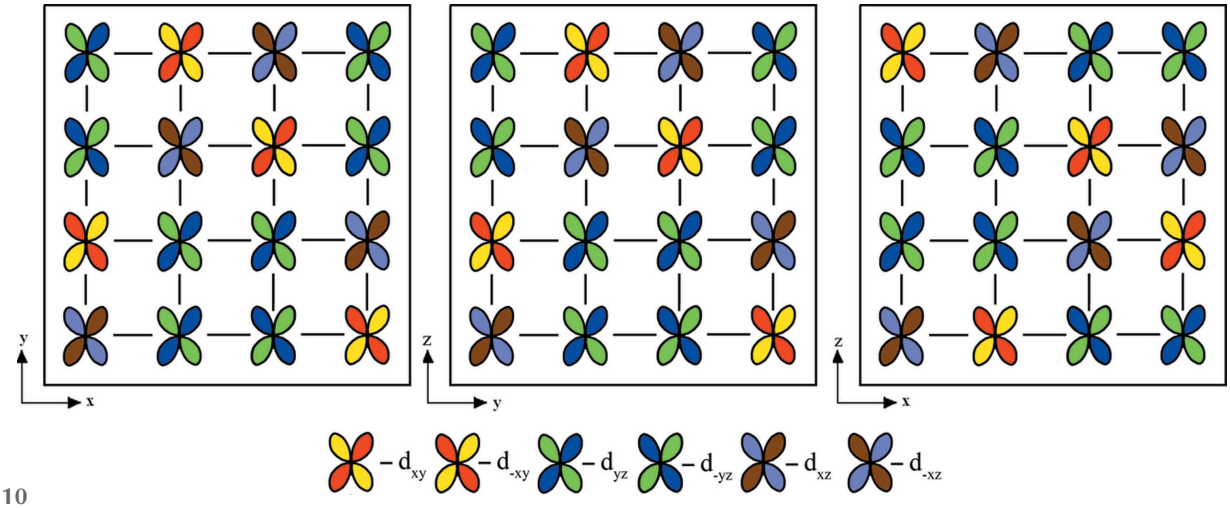

Figure 10
$Na_4Ir_3O_8$ orbital structure in the basis of the initial spinel structure.

Table 2
Phases with binary cation ordering (1:3 type) in Wyckoff position 16*d* of the spinel structure.

Designations for order parameters: $\mathbf{k}_{10} - \varphi$, $\mathbf{k}_{11} - \xi$. The superscript index after the closing parenthesis is the representation number according to Kovalev (1993) and V_0/V is the change of primitive cell volume as a result of the structural phase transition. The superscript index in the structural formula means the type of Wyckoff position according to *International Tables for Crystallography*. If the ordered phase is formed by critical and secondary OPs, the *A* and *B* symbols in the order parameter superscripts are used. They designate positions where cation ordering takes place (*A*-cation ordering takes place in Wyckoff position 8*a*, *B*-cation ordering occurs in Wyckoff position 16*d* of the spinel structure). 'sec' means secondary order parameter.

No.	Order parameters	Space-group symbol	V_0/V	Translations of primitive cell of spinel structure	Structural formula
1	$(\xi, -\xi, \xi)^7$	$R\bar{3}2/m$ (No. 166)	1	$\mathbf{a}_1$, $\mathbf{a}_2$, $\mathbf{a}_3$	$A^c\underline{B^b_{1/2}B^e_{3/2}}X^cX^h_3$
2	$(\varphi, 0, \varphi, 0, \varphi, 0)^3$	$P\bar{4}3m$ (No. 215)	4	$\mathbf{a}_1+\mathbf{a}_2+\mathbf{a}_3$, $2\mathbf{a}_2$, $2\mathbf{a}_3$	$A^a_{1/8}A^c_{3/8}A^e_{1/2}\underline{B^e_{1/2}B^i_{3/2}}X^e_{1/2}X^e_{1/2}X^i_{3/2}X^i_{3/2}$
3	$(\varphi, 0, \varphi, 0, -\varphi, 0)^1$ $(0, \varphi, 0, \varphi, 0, -\varphi)^1$	$P4_332$ (No. 212) $P4_132$ (No. 213)	4	$\mathbf{a}_1+\mathbf{a}_2+\mathbf{a}_3$, $2\mathbf{a}_2$, $2\mathbf{a}_1$	$A^c\underline{B^a_{1/2}B^d_{3/2}}X^cX^e_3$
4	$(0, \varphi, 0, \varphi, 0, -\varphi)^{3,A,B}(\xi)^{4,A}$sec	$P\bar{4}3m$ (No. 215)	4	$\mathbf{a}_1+\mathbf{a}_2+\mathbf{a}_3$, $2\mathbf{a}_2$, $2\mathbf{a}_1$	$\underline{A^a_{1/8}A^c_{3/8}A^e_{1/2}B^e_{1/2}B^i_{3/2}}X^e_{1/2}X^e_{1/2}X^i_{3/2}X^i_{3/2}$
5	$(\xi)^{4,A}(\xi, -\xi, \xi)^{7,B}$	$R3m$ (No. 160)	1	$\mathbf{a}_1$, $\mathbf{a}_2$, $\mathbf{a}_3$	$\underline{A^a_{1/2}A^a_{1/2}B^a_{1/2}B^b_{3/2}}X^a_{1/2}X^a_{1/2}X^b_{3/2}X^b_{3/2}$
6	$(\xi)^{4,A}(0, \varphi, 0, \varphi, 0, -\varphi)^{1,B}$	$P2_13$ (No. 198)	4	$\mathbf{a}_1+\mathbf{a}_2+\mathbf{a}_3$, $2\mathbf{a}_2$, $2\mathbf{a}_1$	$\underline{A^a_{1/2}A^a_{1/2}B^a_{1/2}B^b_{3/2}}X^a_{1/2}X^a_{1/2}X^b_{3/2}X^b_{3/2}$

of microscopic models of the interactions of atoms and interpretation of the physical properties of $Na_4Ir_3O_8$.

3. General case: hyper-kagome order in ordered spinel structures

3.1. Necessary conditions of hyper-kagome order formation

The analysis of theoretical and experimental structure data of $Na_4Ir_3O_8$ allows us to predict the formation of hyper-kagome order in ordered spinels $A_2[BB'_3]O_8$ (type of order 1:3 in 16*d* Wyckoff position). We can formulate three necessary symmetry conditions and one chemical condition for atom hyper-kagome order in structures of low-symmetry ordered spinel modifications:

(i) Critical irreps that generate the onset of the low-symmetry spinel phase should enter into the permutation representation of spinel structure on Wyckoff position 16*d*. This condition means that the low-symmetry spinel phase should be an ordered phase. There are only seven such critical irreps: $\mathbf{k}_{11}(\tau_1)$, $\mathbf{k}_{11}(\tau_7)$, $\mathbf{k}_{10}(\tau_1)$, $\mathbf{k}_{10}(\tau_3)$, $\mathbf{k}_9(\tau_1)$, $\mathbf{k}_9(\tau_4)$, $\mathbf{k}_9(\tau_5)$.

(ii) Wyckoff position 16*d* should be split into two types of Wyckoff positions in the ordered low-symmetry phase. This means that low-symmetry ordered phase structure should be a superstructure with binary cation order. Critical irreps $\mathbf{k}_{11}(\tau_1)$, $\mathbf{k}_9(\tau_1)$, $\mathbf{k}_9(\tau_4)$, $\mathbf{k}_9(\tau_5)$ do not satisfy this condition.

(iii) The ratio of Wyckoff-position multiplicities in the ordered phase structure should be equal to 1:3. Three phases, $R\bar{3}2/m$ ($\mathbf{k}_{11}(\tau_7)$), $P\bar{4}3m$ ($\mathbf{k}_{10}(\tau_3)$), $P4_132$ ($P4_332$) ($\mathbf{k}_{10}(\tau_1)$), satisfy this condition.

Direct sums of irreps entering into the permutation representation of the spinel structure can satisfy conditions (i)–(iii) too.

(iv) Chemical condition. Ordered B' and B atoms should be chemically different. A hyper-kagome sublattice is formed by the B' atom occupying a Wyckoff position with greater multiplicity of position. B 'atoms' may be defects.

$Na_4Ir_3O_8$ is so far the only substance with a unique atomic hyper-kagome order. The formulated conditions make it possible to predict new types of substances with atom hyper-kagome order, as well as to discover this unique atom order in the structure of substances which have repeatedly been investigated before, but where attention was not paid to this atomic order. Examples of new classes of ordered spinels with atom hyper-kagome order are presented below. Substances with structures where the hyper-kagome sublattice is formed by atoms of transition elements have the most interesting physical properties.

3.2. Atom hyper-kagome order in ordered spinel structures

Atom ordering in the spinel structure was investigated previously by group-theoretical methods of phase-transition theory (Talanov & Shirokov, 2014). In this work the possibility of the existence of 320 phases with different types of order in Wyckoff position 16*d* was established. Among these ordered phases there are eight binary superstructures. Only three structures (without taking into account the enantiomorphic modifications) are characterized by the 1:3 order type (phase Nos. 1–3 in Table 2). In addition, cation order of the 1:3 type is also possible in three structures generated by two OPs. These are phases with simultaneous cation ordering in Wyckoff positions 8*a* and 16*d* (phase Nos. 4–6 in Table 2).

Thus cation order of the 1:3 type in Wyckoff position 16*d* is possible only in six types of structures of ordered spinel phases (Table 2), having the space groups: $P4_132$ ($P4_332$), $P2_13$, $R\bar{3}2/m$, $R3m$, $P\bar{4}3m$. Two different types of ordered spinel structures have one space group: $P\bar{4}3m$ (see Table 2). The $P\bar{4}3m$ phase corresponding to row 4 is formed as a result of octahedral cation ordering in Wyckoff position 16*d* (the type of binary order is 1:3) and tetrahedral cations in Wyckoff position 8*a* (the type of ternary order is 1:3:4). The $P\bar{4}3m$ phase corresponding to row 2 is formed as a result of only octahedral cation ordering (the type of binary order is 1:3).

The structure of the $R\bar{3}2/m$ phase is generated by irrep $\mathbf{k}_{11}(\tau_7)$ (Talanov & Shirokov, 2014). This irrep enters into the mechanical representation of the spinel structure on positions 8*a* and 32*e* and enters into the permutation representation of the spinel on positions 16*d* and 32*e*. This means that the low-symmetry phase formation is connected with displacements of tetrahedral cations and anions and also with ordering of octahedral cations and anions (in both cases the types of order are the same, *i.e.* 1:3). The structural formula of a low-symmetry $R\bar{3}2/m$ phase should be $A^{2c}B^{1a}{}_{1/2}B'^{3d}{}_{3/2}X^{2c}X^{6h}{}_3$.

The rhombohedral spinel Ga_3O_3N has $R\bar{3}2/m$ space group (Boyko *et al.*, 2011). When forming the $R\bar{3}2/m$ phase of Ga_3O_3N, not only oxygen and nitrogen ordering takes place but ordering of two from three gallium atoms, occupying Wyckoff positions 1*a* and 3*d*, occurs. The hyper-kagome sublattice is formed by gallium atoms occupying Wyckoff position 3*d*. This sublattice is formed by a network of triangles $[Ga^{3d}{}_3]_n$. Examples of ordered $R\bar{3}2/m$ spinels containing transition atoms in the 3*d* Wyckoff position are as yet unknown.

Among low-symmetry ordered spinel modifications, there are no real examples of phases with $P\bar{4}3m$ and $R3m$ space groups. Therefore low-symmetry spinel structures with these space groups are not considered in this work. From these six types of predicted structures, there are examples of only two of them in experimentally discovered substances.

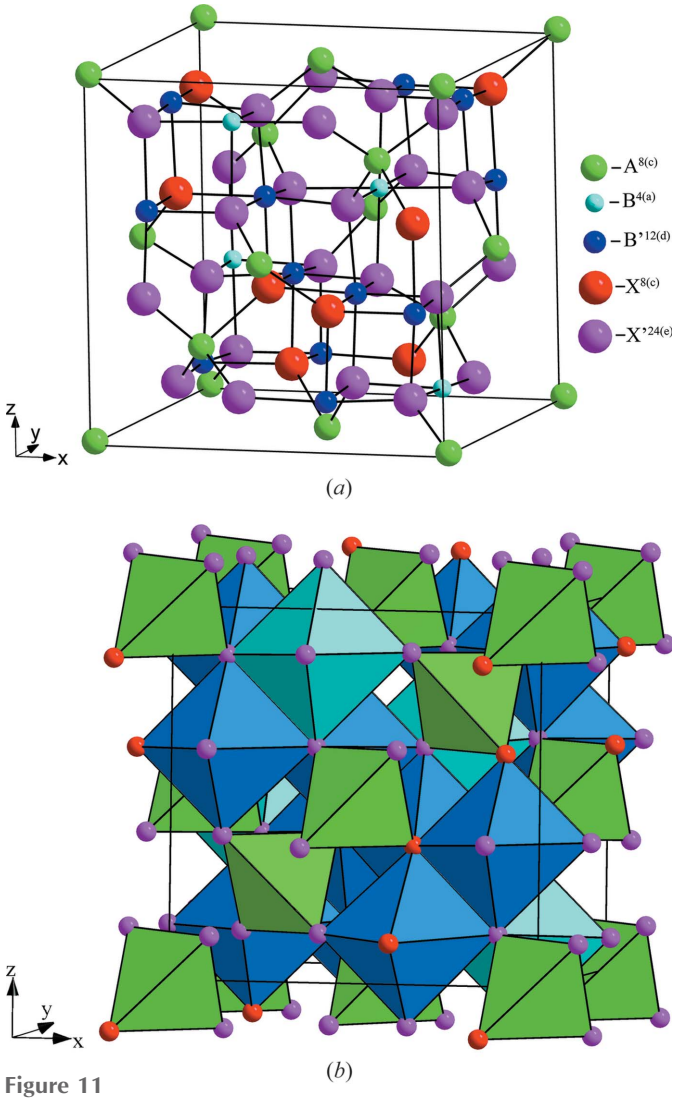

Figure 11
Structure of the low-symmetry ordered $P4_132$ modification of spinel. Atom representation (*a*), polyhedral representation (*b*). In the centre of a blue octahedra is atom B^{4b}, in the centre of the dark blue octahedra is atom B'^{12d}.

3.3. Atom hyper-kagome order in the $P4_132$ ($P4_332$) spinel structure

$P4_132$ ($P4_332$) spinel phases are a widespread type of a low-symmetry ordered enantiomorphic modification of the spinel structure. They are formed as a result of phase transitions from spinel structures. These phases are generated by critical irrep $\mathbf{k}_{10}(\tau_1)$ (Talanov & Shirokov, 2012, 2014). Irrep $\mathbf{k}_{10}(\tau_1)$ enters into both permutation (on Wyckoff positions 16*d* and 32*e*) and mechanical (on Wyckoff positions 8*a*, 16*d*, 32*e*) representations of the spinel structure. Therefore the lowering of crystal symmetry is due to displacements of all atom types and ordering of octahedral cations and anions (in both cases the type of order is 1:3). Theoretical results show that atoms A^{8c} are located in weakly distorted tetrahedra, atoms B'^{12d} are in distorted octahedra and atoms B^{4b} are present in regular octahedra (Fig. 11). The structure formula of the low-symmetry phases can be given as follows: $A^{8c}{}_2B^{4b}B'^{12d}{}_3X^{8c}{}_2X^{24e}{}_6$ (Talanov & Shirokov, 2014).

The hyper-kagome sublattice in the $P4_132$ ($P4_332$)-phase structure is formed by triangles $[B'^{12d}{}_3]_n$ (Fig. 12). Each of these sublattices is topologically the same as the hyper-kagome sublattice in the $Na_4Ir_3O_8$ structure. However, the surroundings of hyper-kagome sublattices in the $P4_132$ ($P4_332$)-phase structures and in the $Na_4Ir_3O_8$ structure are different. Examples of substances with $P4_132$- and $P4_332$-phase ordered structures are given in Table 3. In structures of these substances there are hyper-kagome sublattices.

We would like to draw attention to lacunar ordered spinels $Zn_2Mn_3O_8$, $ZnMGe_3O_8$ (M = Mn^{2+}, Mg^{2+}), $M_2Ge_3O_8$ (M =

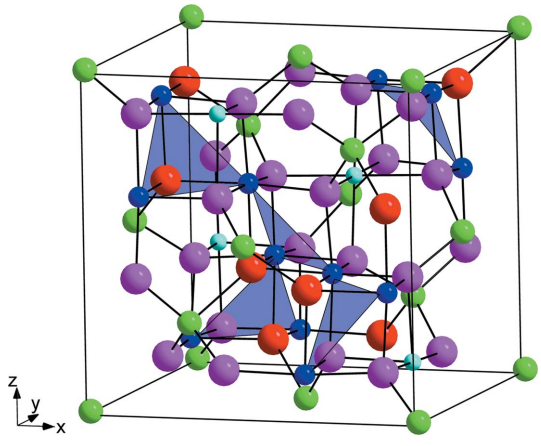

Figure 12
Fragment of the hyper-kagome sublattice of the $P4_132$-phase structure. This fragment is formed by triangles $[B'^{12d}{}_3]_n$ (dark blue atoms).

Zn^{2+}, Co^{2+}), $ZnMTi_3O_8$ (M = Mn^{2+}, Cd^{2+}), $M_2Ti_3O_8$ (M = Zn^{2+}, Mn^{2+}, Co^{2+}, Cd^{2+}), $V_2Co_3O_8$ (Joubert & Durif, 1964*a*,*b*; Steinikeb & Wallis, 1997) (Table 3). The difference between the $Na_4Ir_3O_8$ structure and the $P4_132$ ($P4_332$)-phase structure in lacunar spinels is that one vertex (B^{4b}) in each tetrahedron $[B^{4b}B'^{12d}{}_3]$ is unoccupied by atoms, *i.e.* it is vacant. The remaining vertices form a hyper-kagome sublattice built from triangles $[B'^{12d}{}_3]_n$. The structure formula of ordered lacunar spinels should be $A^{8c}{}_2\square\,{}^{4b}B'^{12d}{}_3X^{8c}{}_2X^{24e}{}_6$. The symbol □ stands for unoccupied sites of the ordered spinel structures.

The theoretical structure of lacunar ordered spinels is shown in Fig. 13. The hyper-kagome sublattice in the structure of these substances is presented in Fig. 13 in an idealized form.

3.4. Phase diagram of the $P4_132$ ($P4_332$) phase with atom hyper-kagome order

The six-component OP, transformed according to irrep $\mathbf{k}_{10}(\tau_1)$ of $Fd\bar{3}m$ group symmetry, forms a point group of order 192 in six-dimensional space. The OP transformation properties are given by the following generator matrices:

$$a_1\colon \begin{pmatrix} -1 & & & & & \\ & -1 & & & & \\ & & -1 & & & \\ & & & -1 & & \\ & & & & 1 & \\ & & & & & 1 \end{pmatrix}, \quad a_2\colon \begin{pmatrix} -1 & & & & & \\ & -1 & & & & \\ & & 1 & & & \\ & & & 1 & & \\ & & & & -1 & \\ & & & & & -1 \end{pmatrix}, \quad (h_2|0)\colon \begin{pmatrix} 1 & & & & & \\ & -1 & & & & \\ & & -1 & & & \\ & & & 1 & & \\ & & & & -1 & \\ & & & & & -1 \end{pmatrix}, \quad (h_3|0)\colon \begin{pmatrix} -1 & & & & & \\ & 1 & & & & \\ & & -1 & & & \\ & & & -1 & & \\ & & & & 1 & \\ & & & & & -1 \end{pmatrix},$$

$$(h_5|0)\colon \begin{pmatrix} & & 1 & & & \\ & & & & & 1 \\ 1 & & & & & \\ & 1 & & & & \\ & & & 1 & & \\ & & & & 1 & \end{pmatrix},$$

$$(h_{13}|\tau\tau\tau)\colon \begin{pmatrix} 1 & & & & & \\ & 1 & & & & \\ & & & & 1 & \\ & & & & & 1 \\ & & 1 & & & \\ & & & 1 & & \end{pmatrix},$$

$$(h_{25}|\tau\tau\tau)\colon \begin{pmatrix} & 1 & & & & \\ 1 & & & & & \\ & & & 1 & & \\ & & 1 & & & \\ & & & & & 1 \\ & & & & 1 & \end{pmatrix}, \qquad (8)$$

where the main diagonal is written in a column, h_i is a rotation part of the symmetry element $g_i = \{h_i|\tau_i\}$ of the $Fd\bar{3}m$ group, τ_i is the accompanying nontrivial translation of h_i, and a_1, a_2 are basic vectors of the primitive cell. In equation (8) the generators of irrep $\mathbf{k}_{10}(\tau_1)$ of $Fd\bar{3}m$ group symmetry are given. The remaining irrep $\mathbf{k}_{10}(\tau_1)$ matrices corresponding to other elements of $Fd\bar{3}m$ group symmetry can be obtained as a result of multiplication of the above-mentioned matrices. For example, the matrix of representation corresponding to translation a_3 is the result of the multiplication of the a_1 and a_2 matrices. Designations for symmetry elements of the $Fd\bar{3}m$ space group are given according to Kovalev (1993). Irrep $\mathbf{k}_{10}(\tau_1)$ corresponds to irrep $X3$ (Stokes & Hatch, 2007). The relationship between the OPs is the following: $\varphi_1 = \eta_1 + \eta_2$, $\varphi_2 = -\eta_1 + \eta_2$, $\varphi_3 = \eta_5 + \eta_6$, $\varphi_4 = -\eta_5 + \eta_6$, $\varphi_5 = \eta_3 + \eta_4$, $\varphi_6 = -\eta_3 + \eta_4$, where η_i are transformed according to irrep $X3$.

The basis of invariants of the thermodynamic potential consists of 13 monomials that do not exceed the ninth degree:

$$\begin{aligned}
J_1 &= \varphi_1^2 + \varphi_2^2 + \varphi_3^2 + \varphi_4^2 + \varphi_5^2 + \varphi_6^2,\\
J_2 &= \varphi_1\varphi_3\varphi_5 + \varphi_2\varphi_4\varphi_6,\\
J_3 &= \varphi_1^2\varphi_2^2 + \varphi_3^2\varphi_4^2 + \varphi_5^2\varphi_6^2,\\
J_4 &= \varphi_1^2\varphi_3^2 + \varphi_1^2\varphi_5^2 + \varphi_2^2\varphi_4^2 + \varphi_2^2\varphi_6^2 + \varphi_3^2\varphi_5^2 + \varphi_4^2\varphi_6^2,\\
J_5 &= \varphi_1^2\varphi_4^2 + \varphi_1^2\varphi_6^2 + \varphi_2^2\varphi_3^2 + \varphi_2^2\varphi_5^2 + \varphi_3^2\varphi_6^2 + \varphi_4^2\varphi_5^2,\\
J_6 &= \varphi_1\varphi_2^2\varphi_3\varphi_5 + \varphi_1^2\varphi_2\varphi_4\varphi_6 + \varphi_1\varphi_3\varphi_4^2\varphi_5 + \varphi_1\varphi_3\varphi_5\varphi_6^2\\
&\quad + \varphi_2\varphi_3^2\varphi_4\varphi_6 + \varphi_2\varphi_4\varphi_5^2\varphi_6,\\
J_7 &= \varphi_1^2\varphi_2^2\varphi_3^2 + \varphi_1^2\varphi_2^2\varphi_4^2 + \varphi_1^2\varphi_2^2\varphi_5^2 + \varphi_1^2\varphi_2^2\varphi_6^2\\
&\quad + \varphi_1^2\varphi_3^2\varphi_4^2 + \varphi_1^2\varphi_5^2\varphi_6^2 + \varphi_2^2\varphi_3^2\varphi_4^2 + \varphi_2^2\varphi_5^2\varphi_6^2\\
&\quad + \varphi_3^2\varphi_4^2\varphi_5^2 + \varphi_3^2\varphi_4^2\varphi_6^2 + \varphi_3^2\varphi_5^2\varphi_6^2 + \varphi_4^2\varphi_5^2\varphi_6^2,\\
J_8 &= \varphi_1^2\varphi_3^2\varphi_6^2 + \varphi_1^2\varphi_4^2\varphi_5^2 + \varphi_1^2\varphi_4^2\varphi_6^2 + \varphi_2^2\varphi_3^2\varphi_5^2\\
&\quad + \varphi_2^2\varphi_3^2\varphi_6^2 + \varphi_2^2\varphi_4^2\varphi_5^2,\\
J_9 &= \varphi_1\varphi_2\varphi_3\varphi_4\varphi_5\varphi_6,\\
J_{10} &= \varphi_1\varphi_2^2\varphi_3\varphi_4^2\varphi_5 + \varphi_1^2\varphi_2\varphi_3^2\varphi_4\varphi_6 + \varphi_1\varphi_2^2\varphi_3\varphi_5\varphi_6^2\\
&\quad + \varphi_1^2\varphi_2\varphi_4\varphi_5^2\varphi_6 + \varphi_1\varphi_3\varphi_4^2\varphi_5^2\varphi_6 + \varphi_2\varphi_3^2\varphi_4\varphi_5^2\varphi_6,\\
J_{11} &= \varphi_1^2\varphi_2^2\varphi_3^2\varphi_4^2 + \varphi_1^2\varphi_2^2\varphi_5^2\varphi_6^2 + \varphi_3^2\varphi_4^2\varphi_5^2\varphi_6^2,\\
J_{12} &= \varphi_1^2\varphi_2^2\varphi_3^2\varphi_6^2 + \varphi_1^2\varphi_2^2\varphi_4^2\varphi_5^2 + \varphi_1^2\varphi_3^2\varphi_4^2\varphi_6^2\\
&\quad + \varphi_1^2\varphi_2^2\varphi_5^2\varphi_6^2 + \varphi_2^2\varphi_3^2\varphi_4^2\varphi_5^2 + \varphi_2^2\varphi_3^2\varphi_5^2\varphi_6^2,\\
J_{13} &= \varphi_1\varphi_2^2\varphi_3\varphi_4^2\varphi_5^3 + \varphi_1^2\varphi_2\varphi_3^2\varphi_4\varphi_6^3 + \varphi_1\varphi_2^2\varphi_3^3\varphi_5\varphi_6^2\\
&\quad + \varphi_1^2\varphi_2\varphi_4^3\varphi_5^2\varphi_6 + \varphi_1^3\varphi_3\varphi_4^2\varphi_5\varphi_6^2 + \varphi_2^3\varphi_3^2\varphi_4\varphi_5^2\varphi_6. \qquad (9)
\end{aligned}$$

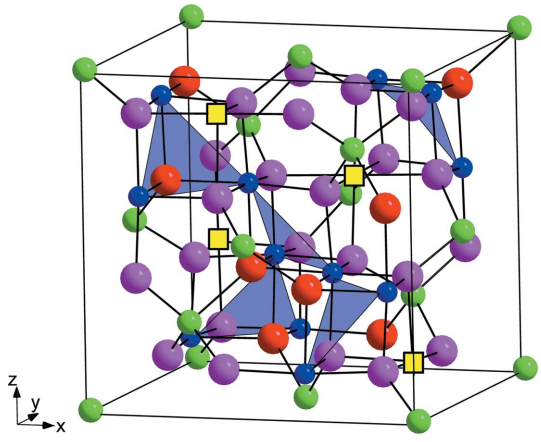

Figure 13
Lacunar ordered $P4_132$ phase of spinel. Atoms B'^{12d} forming the hyper-kagome sublattice are designated by dark blue colour, defects are designated by yellow squares.

Table 3
$P4_132$ ($P4_332$) spinel phases with cation ordering of 1:3 type.

Compositions of substances	Distribution of cations on Wyckoff positions			Cations forming hyper-kagome sublattices	References
	8*c*	4*b*	12*d*		
$Zn_3Ni_2TeO_8$	$2Zn^{2+}$	Te^{6+}	Zn^{2+} $2Ni^{2+}$	Zn^{2+}, Ni^{2+}	Bayer (1967)
$Zn_2Co_3TeO_8$	$2Zn^{2+}$	Te^{6+}	$3Co^{2+}$	Co^{2+}	Bayer (1967)
$CuMg_{0.5}Mn_{1.5}O_4$	Cu^{+}	$0.5Mg^{2+}$	$1.5Mn^{4+}$	Mn^{4+}	Blasse (1966); Vandenberghe *et al.* (1976)
$Cu_{1.5}Mn_{1.5}O_4$	Cu^{+}	0.5Cu	$1.5Mn^{4+}$	Mn^{4+}	Blasse (1966); Vandenberghe *et al.* (1976)
$Zn_2Mn_3O_8$	$2Zn^{2+}$		$3Mn^{4+}$	Mn^{4+}	Joubert & Durif (1964*a*)
$ZnMGe_3O_8$ (M = Mn^{2+}, Mg^{2+})	Zn^{2+} M^{2+}		$3Ge^{4+}$	Ge^{4+}	Joubert & Durif (1964*a*)
$M_2Ge_3O_8$ (M = Zn^{2+}, Co^{2+})	$2M^{2+}$		$3Ge^{4+}$	Ge^{4+}	Joubert & Durif (1964*a*)
$ZnMTi_3O_8$ (M = Mn^{2+}, Cd^{2+})	Zn^{2+} M^{2+}		$3Ti^{4+}$	Ti^{4+}	Joubert & Durif (1964*a*)
$M_2Ti_3O_8$ (M = Zn^{2+}, Mn^{2+}, Co^{2+}, Cd^{2+})	$2M^{2+}$		$3Ti^{4+}$	Ti^{4+}	Joubert & Durif (1964*a*)
$V_2Co_3O_8$	$2V^{5+}$		$3Co^{2+}$	Co^{2+}	Joubert & Durif (1964*b*)
$Zn_2Ti_3O_8$	$2Zn^{2+}$		$3Ti^{4+}$	Ti^{4+}	Steinikeb & Wallis (1997)
$Li_2CoTi_3O_8$ (for i = 1 in the formula $[A_{2-i}B_i]^{8c}$ $[A_iB_{1-i}]^{4b}[B'_3]^{12d}O_8$)	Li^{+} Co^{2+}	Li^{+}	$3Ti^{4+}$	Ti^{4+}	Reeves *et al.* (2007)
$Li_2NiGe_3O_8$ (at room temperature)	$2Li^{+}$	Ni^{2+}	$3Ge^{4+}$	Ge^{4+}	Kawai *et al.* (1998); Reeves-McLaren *et al.* (2011)
$Li_2ZnGe_3O_8$ (at room temperature)	Li^{+} Zn^{2+}	Li^{+}	$3Ge^{4+}$	Ge^{4+}	Kawai *et al.* (1998); Reeves-McLaren *et al.* (2011)
$LiNi_{0.5}Mn_{1.5}O_4$, $LiNi_{0.5}Mn_{1.5}O_{4-\delta}$	Li^{+}	Ni^{2+} Li^{+}	$1.5Mn^{4+}$	Mn^{4+}	Wang *et al.* (2011); Kim *et al.* (2004); Strobel *et al.* (2003)
$LiFe_5O_8$	$2Fe^{3+}$	Li^{+}	$3Fe^{3+}$	Fe^{3+}	Boyko *et al.* (2011); O'Keeffe & Partin (1994)
LiM_5O_8 (M = Al^{3+}, Ga^{3+})	$2M^{3+}$	Li^{+}	$3M^{3+}$	M^{3+}	Ahman *et al.* (1996); Datta & Roy (1963); Tarte & Collongues (1964); Nageswara Rao & Ghose (1986)
$Li_2Mn_3MgO_8$	Li^{+}	Mg^{2+}	$3Mn^{4+}$	Mn^{4+}	Strobel *et al.* (2000)
$Li_2MTi_3O_8$ (M = Co^{2+}, Zn^{2+}, Cd^{2+})	Li^{+} M^{2+}	Li^{+}	$3Ti^{4+}$	Ti^{4+}	Joubert & Durif (1961); Reeves *et al.* (2007)
$Na_3Ir_3O_8$	Na^{+}	Na^{+}	$3Ir^{4.33+}$	$Ir^{4.33+}$	Takayama *et al.* (2001); Pröpper *et al.* (2014)

The invariants basis was constructed using the algorithm described in Shirokov (2011). The computer program was written using the *Maple* mathematical package.

As in the thermodynamic potential (10) there is an invariant of the third degree on components of the OP; any phenomenological model of a phase transition with the OP which has symmetry (8) will describe only phase transitions of the first order between the high-symmetry phase and low-symmetry phases bordering it. A phenomenological thermodynamic model of phase transitions will be built taking into account thermodynamic potential stability (Prokhorov *et al.*, 1984; Kut'in *et al.*, 1991; Poston & Stewart, 1978; Arnold, 1992).

The term 'stable' refers to the potential that allows us to construct a phase diagram that does not change on the appearance of a small external perturbation to the potential. A small perturbation should lead to only small quantitative changes without changing the type and number of phases and the topology of the phase diagrams.

The investigation directed towards stability is made locally near the point of instability, which is determined in the phenomenological theory, at least, by vanishing the coefficient at the square of the order parameter. For the six-component OP, transformed according to irrep $\mathbf{k}_{10}(\tau_1)$, the requirement of stability leads to the potential of the sixth degree on OP components. The stable potential has the form

$$\begin{aligned} F = {} & \underline{a_1J_1 + b_2J_2 + c_{11}J_1^2} \\ & + c_3J_3 + c_4J_4 + c_5J_5 + d_{12}J_1J_2 + d_6J_6 \\ & + f_{111}J_1^3 + f_{13}J_1J_3 + f_{14}J_1J_4 + f_{15}J_1J_5 \\ & + f_{22}J_2^2 + f_7J_7 + f_8J_8 + f_9J_9. \end{aligned} \quad (10)$$

In expression (10) the underlined terms define the multicritical point ($a_1 = 0$, $b_2 = 0$, $c_{11} = 0$), near which potential (10) is stable. A typical phase diagram for potential (10) in the plane (a_1, b_2) is shown in Fig. 14. All coefficients of the potential (10) that are not defined in Fig. 14 are positive. The high-symmetry $Fd\bar{3}m$ phase with zero OP (0, 0, 0, 0, 0, 0) at $c_{11} > 0$ (Fig. 14*a*) is bordered by the low-symmetry $P4_132$ phase with OP direction (0, φ, 0, φ, 0, $-\varphi$) along the lines of phase transition of the first order everywhere except the point ($a_1 = 0$, $b_2 = 0$). At this point a phase transition of the second order into the phase $P4_122$ with OP direction (0, 0, 0, 0, 0, φ) is possible. Since this phase transition can occur only at a single point, the probability of such a transition in the plane of the thermodynamic parameters (a_1, b_2) is extremely small. Therefore one can consider that at $c_{11} > 0$, a phase transition of

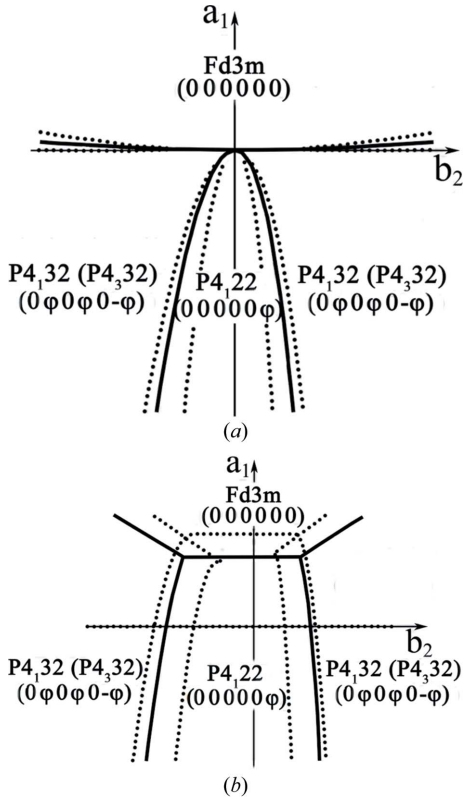

Figure 14
Phase diagram described by potential (10). The diagram for the case where $c_{11} > 0$ is shown in (*a*) and the diagram for the case where $c_{11} < 0$ is shown in (*b*). The solid line is a line of phase transition of the first order, dotted lines restrict the fields of metastable phases.

the first order from the $Fd\bar{3}m$ high-symmetry phase into the $P4_132$ phase is most probable. At $c_{11} < 0$ (Fig. 14*b*) and at small b_2, a large field exists on the phase diagram, at the phase boundary of the first order between the high-symmetry $Fd\bar{3}m$ phase and the low-symmetry $P4_122$ phase. A phase transition from the high-symmetry phase into the $P4_132$ phase on the phase diagram is possible both at $b_2 > 0$ and at $b_2 < 0$. If the term of fifth degree on φ were absent in the thermodynamic potential (10) (if $d_{12} = 0$), then $P4_132$ phases on the left and on the right on the phase diagrams (Fig. 14) would differ from each other only by the sign φ, and the diagrams would be symmetrical. Such phases are called anti-isostructure ones (Gufan, 1982; Talanov & Paschenko, 1995; Sakhnenko & Talanov, 1979, 1980; Talanov & Mukovnin, 2013; Mukovnin & Talanov, 2014). However, at $d_{12} \neq 0$, these phases differ not only by the OP φ sign but also by its absolute meaning.

Thus the appearance on phase diagrams of $P4_132$ phases should take place as a result of phase transitions of the first order. Therefore the formation of hyper-kagome sublattices in these phase structures must take place as a result of the fundamental reconstruction of the initial high-symmetry parent structure.

3.5. Atom hyper-kagome order in the $P2_13$-phase structure

The structure of the $P2_13$ phase is generated by two OPs: a one-component OP (ξ) transformed according to irrep $\mathbf{k}_{11}(\tau_4)$ ($\tau_4 = A_{2u}$) and a six-component OP with direction (0, φ, 0, φ, 0, $-\varphi$) transformed according to irrep $\mathbf{k}_{10}(\tau_1)$ (Talanov & Shirokov, 2013*a*,*b*). These two OPs form a point group of order 192 in seven-dimensional order space.

The transformational properties of the OP are determined by the seven-dimensional matrices, where a six-dimensional matrix (8) is added to matrices of the one-dimensional representation $\mathbf{k}_{11}(\tau_4)$. Such an OP generates 24 low-symmetry ordered phases (Talanov & Shirokov, 2013*a*,*b*).

The mechanism of the formation of the low-symmetry phase formed according to the representation $\mathbf{k}_{10}(\tau_1) + \mathbf{k}_{11}(\tau_4)$ is the most complex. This mechanism has the following features: (i) cation binary orderings in tetrahedral Wyckoff positions 8*a* (1:1 type) and in octahedral Wyckoff position 16*d* (1:3 type) of the initial spinel structure; (ii) quaternary anion ordering of 1:1:3:3 type in the initial phase structure; (iii) displacements of all types of atoms.

The structure formula of the $P2_13$ phase can be shown as follows: $(A^{4a}{}_{1/2}A'^{4a}{}_{1/2})[B^{4a}{}_{1/2}B'^{12b}{}_{3/2}]X^{12b}X'^{12b}X^{4a}X'^{4a}$ (Talanov & Shirokov, 2013*a*,*b*). Only one example of a superstructure with simultaneous cation ordering in Wyckoff positions 8*a* and 16*d* of spinel structure is known. This is the ordered phase of the $Li_2ZnMn_3O_8$ spinel (Lee *et al.*, 2002; Joubert & Durif, 1964*c*; Chen *et al.*, 1986).

Neutron and X-ray diffraction experimental data on the $Li_2ZnMn_3O_8$ structure agree with the proposed structural formula given. Using the obtained scalar and vector basis functions of the critical irrep, we constructed a structural model of the low-symmetry phase. In Fig. 15 the obtained structure of the ordered $P2_13$ phase is shown.

A network of triangles $[B'^{12b}{}_3]_n$ in the $P2_13$-phase structure forms a hyper-kagome sublattice (Fig. 16). The hyper-kagome sublattice in the $P2_13$ phase is exactly the same as in the $P4_132$ ($P4_332$)-phase structure. In the $Li_2ZnMn_3O_8$ ordered spinel structure, Mn^{4+} ions form a hyper-kagome sublattice.

3.6. Phase diagram of the $P2_13$ phase with atom hyper-kagome order

To determine the thermodynamic conditions of forming the $P2_13$ phase with atom hyper-kagome order, it is necessary to build a most probable phase diagram.

The basis of invariants for thermodynamic potential (11) consists of 21 monomials with the maximum degree of ten. The six-component OP has a third-degree invariant; therefore, phase transitions with this OP can only be of the first order between the high-symmetry phase and with low-symmetry phases bordering it. Let us write the sixth-degree stable potential in such a way:

$$\begin{aligned} F = {} & a_1J_1 + b_1J_2 + v_3J_3 + c_{11}J_1^2 + c_{12}J_1J_2 + c_{22}J_2^2 + c_4J_4 \\ & + c_5J_5 + c_6J_6 + d_{13}J_1J_3 + d_{23}J_2J_3 + d_7J_7 + d_8J_8 \\ & + f_{111}J_1^3 + f_{112}J_1^2J_2 + f_{122}J_1J_2^2 + f_{222}J_2^3 + f_{14}J_1J_4 \\ & + f_{24}J_2J_4 + f_{15}J_1J_5 + f_{25}J_2J_5 + f_{16}J_1J_6 \\ & + f_{26}J_2J_6 + f_{33}J_3^2 + f_9J_9 + f_{10}J_{10} + f_{11}J_{11}. \end{aligned} \quad (11)$$

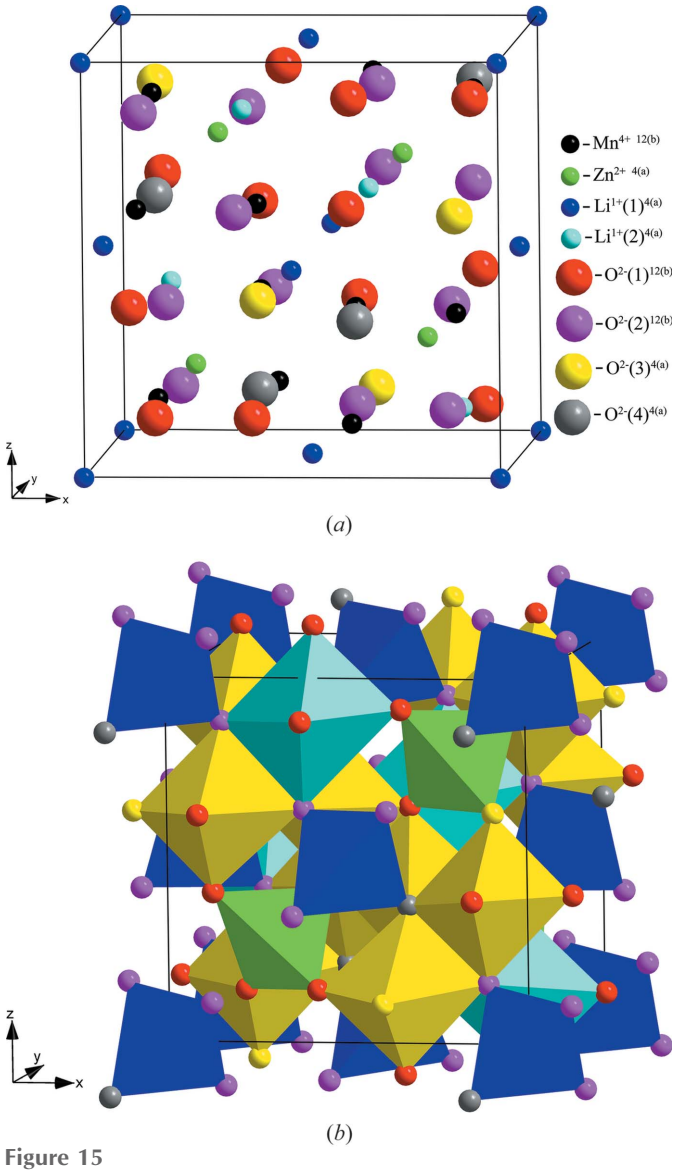

Figure 15
Atom representation of $Li_2ZnMn_3O_8$ structure (*a*), polyhedral model of the ordered structure in the form of ($Li1O_4$) (dark blue) and ($Zn1O_4$) (green) tetrahedra and ($Li2O_6$) (blue) and (MnO_6) (yellow) octahedra (*b*).

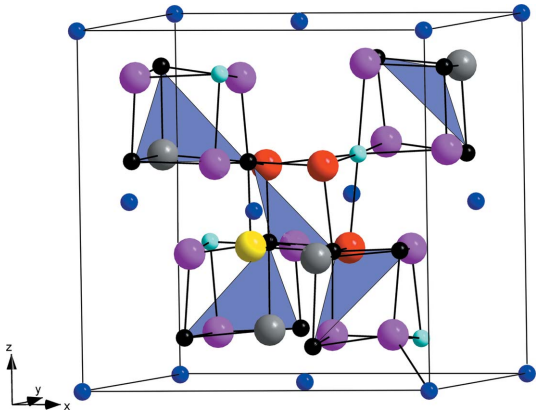

Figure 16
Fragment of the hyper-kagome sublattice in the ordered phase structure.

The invariants composed of the OP component in equation (11) can be written as

$$
\begin{aligned}
J_1 &= \varphi_1^2 + \varphi_2^2 + \varphi_3^2 + \varphi_4^2 + \varphi_5^2 + \varphi_6^2,\\
J_2 &= \xi^2,\\
J_3 &= \varphi_1\varphi_3\varphi_5 + \varphi_2\varphi_4\varphi_6,\\
J_4 &= \varphi_1^2\varphi_2^2 + \varphi_3^2\varphi_4^2 + \varphi_5^2\varphi_6^2,\\
J_5 &= \varphi_1^2\varphi_3^2 + \varphi_1^2\varphi_5^2 + \varphi_2^2\varphi_4^2 + \varphi_2^2\varphi_6^2 + \varphi_3^2\varphi_5^2 + \varphi_4^2\varphi_6^2,\\
J_6 &= \varphi_1^2\varphi_4^2 + \varphi_1^2\varphi_6^2 + \varphi_2^2\varphi_3^2 + \varphi_2^2\varphi_5^2 + \varphi_3^2\varphi_6^2 + \varphi_4^2\varphi_5^2,\\
J_7 &= \varphi_1\varphi_2^2\varphi_3\varphi_5 + \varphi_1^2\varphi_2\varphi_4\varphi_6 + \varphi_1\varphi_3\varphi_4^2\varphi_5 + \varphi_1\varphi_3\varphi_5\varphi_6^2\\
&\quad + \varphi_2\varphi_3^2\varphi_4\varphi_6 + \varphi_2\varphi_4\varphi_5^2\varphi_6,\\
J_8 &= \xi(\varphi_1^2\varphi_4^2 + \varphi_2^2\varphi_5^2 + \varphi_3^2\varphi_6^2 - \varphi_1^2\varphi_6^2 - \varphi_4^2\varphi_5^2 - \varphi_2^2\varphi_3^2),\\
J_9 &= \varphi_1^2\varphi_2^2\varphi_3^2 + \varphi_1^2\varphi_2^2\varphi_4^2 + \varphi_1^2\varphi_2^2\varphi_5^2 + \varphi_1^2\varphi_2^2\varphi_6^2\\
&\quad + \varphi_1^2\varphi_3^2\varphi_4^2 + \varphi_1^2\varphi_5^2\varphi_6^2 + \varphi_2^2\varphi_3^2\varphi_4^2 + \varphi_2^2\varphi_5^2\varphi_6^2\\
&\quad + \varphi_3^2\varphi_4^2\varphi_5^2 + \varphi_3^2\varphi_4^2\varphi_6^2 + \varphi_3^2\varphi_5^2\varphi_6^2 + \varphi_4^2\varphi_5^2\varphi_6^2,\\
J_{10} &= \varphi_1^2\varphi_3^2\varphi_6^2 + \varphi_1^2\varphi_4^2\varphi_5^2 + \varphi_1^2\varphi_4^2\varphi_6^2 + \varphi_2^2\varphi_3^2\varphi_5^2\\
&\quad + \varphi_2^2\varphi_3^2\varphi_6^2 + \varphi_2^2\varphi_4^2\varphi_5^2,\\
J_{11} &= \varphi_1\varphi_2\varphi_3\varphi_4\varphi_5\varphi_6,
\end{aligned}
$$

where φ and ξ transform by $\mathbf{k}_{10}(\tau_1)$ and $\mathbf{k}_{11}(\tau_4)$, respectively.

Phase diagrams described by the potential (11) are multivariant and complex. Their appearance depends on the ratio of the phenomenological coefficients in the thermodynamic potential. A simple phase diagram for the special case when all the coefficients are positive, except for $c_{11} < 0$, and the condition $c_{11}c_{22} - {c_{12}}^2 > 0$ is satisfied is shown in Fig. 17.

From the phase diagram it is seen that the ordered $P2_13$ phase, the structure of which contains a hyper-kagome sublattice, can be formed only through intermediate phases with space groups $F43m$, $P4_132$ ($P4_332$), $P4_122$ ($P4_322$) and $C222_1$ as a result of a phase transition of the first order. The $P2_13$ phase cannot be formed directly from the cubic spinel phase. This means that in this case the formation of a hyper-kagome sublattice in the $P2_13$-phase structure occurs in a complicated way from intermediate phase structures by their fundamental reconstructions.

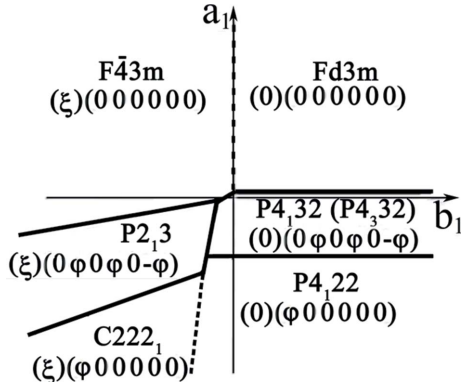

Figure 17
Phase diagram described by potential (11) at $c_{11} < 0$ and $c_{11}c_{22} - {c_{12}}^2 > 0$; the lines of the first- and second-order transitions are indicated by solid and dashed lines, respectively.

4. Conclusions

For the first time within the framework of a unified approach, based on group-theoretical and thermodynamic methods of modern phase-transition theory, the study of unique hyper-kagome order in structures of spinel-like $Na_4Ir_3O_8$ and ordered spinels has been carried out.

(i) Based on the concepts of archetype we have established the spinel-like archetype structure of $Na_4Ir_3O_8$ – $[Na_{1/2}Ir_{3/2}]^{16d}[Na_{3/2}]^{16c}O^{32e}{}_4$ (space group $Fd\bar{3}m$).

(ii) It is shown that the critical irrep, generating the appearance of the $P4_132$ ($P4_332$) phase from a high-symmetry spinel-like archetype phase with space group $Fd\bar{3}m$, is the six-dimensional irrep $\boldsymbol{\kappa}_{10}(\tau_1)$.

(iii) It is shown that the derived $Na_4Ir_3O_8$ structure is formed as a result of atom displacements and orderings of sodium, iridium and oxygen (1:3 type). Ordered phase formation is also accompanied by d_{xy}, d_{xz}, d_{yz} orbital ordering of Ir atoms.

(iv) For the first time it is found that the metal atoms form two networks of tetrahedra with different chemical compositions: $[Na^{12d}{}_3Na^{4a}]_n$ and $[Ir^{12d}{}_3Na^{4b}]_n$. From these networks, two different hyper-kagome sublattices in the $Na_4Ir_3O_8$ structure are formed. However, the physical properties of $Na_4Ir_3O_8$ are associated with the network of $[Ir^{12d}{}_3Na^{4b}]_n$ tetrahedra. Unique atomic order, the hyper-kagome sublattice, is formed by magnetic Ir atoms from this network. Thus, the hyper-kagome sublattice is a network of $[Ir^{12d}{}_3]_n$ triangles from Ir atoms.

(v) It is shown that in hyper-kagome sublattices in $Na_4Ir_3O_8$ one can select the module from the three intersecting loops of Ir—Ir chemical bonds. The shortest closed loop is a metal cluster consisting of ten Ir atoms (this cluster is a decagon).

(vi) The detailed theoretical study of the $Na_4Ir_3O_8$ structure allowed us to formulate conditions for the existence of hyper-kagome sublattices and predict them in six types of structures of ordered spinel phases (Table 2), having space groups $P4_132$ ($P4_332$), $P2_13$, $R\bar{3}2/m$, $R3m$ and $P\bar{4}3m$.

(vii) Examples of substances from six predicted types of structures are known only for two types of structures [with space groups $P4_132$ ($P4_332$) and $P2_13$] which form a hyper-kagome sublattice and contain magnetic ions. These structures have been studied in this work.

The hyper-kagome sublattice in the $P4_132$ ($P4_332$) phases, having structural formula $A^{8c}{}_2B^{4b}B'^{12d}{}_3X^{8c}{}_2X^{24e}{}_6$, is formed by triangles $[B^{12d}{}_3]_n$. Topologically, this hyper-kagome sublattice is the same as in the $Na_4Ir_3O_8$ structure.

The hyper-kagome sublattice in the $P2_13$ phase, having structural formula $(A^{4a}{}_{1/2}A'^{4a}{}_{1/2})[B^{4a}{}_{1/2}B'^{12b}{}_{3/2}]$-$X^{12b}X'^{12b}X^{4a}X'^{4a}$, is formed by triangles $[B'^{12b}{}_3]_n$. In the $P2_13$-phase structure the hyper-kagome sublattice is topologically the same as in the $Na_4Ir_3O_8$ and $P4_132$ ($P4_332$)-phase structures. But the nearest atom surrounding of these sublattices is different in all these cases.

(viii) The global pattern of changes in the phase states was considered within the model, taking into account the terms in the free energy up to the sixth degree in the OP components in the Landau theory of phase transitions. Thermodynamic analysis showed that the hyper-kagome sublattices in the $P4_132$ ($P4_332$) phases are formed from the initial archetype phase in $Na_4Ir_3O_8$ and the parent spinel phase in ordered phases only as a result of first-order phase transitions. It is important to underline that the hyper-kagome sublattice in the $P2_13$ phases is not formed directly from the cubic spinel structure, but is formed from intermediate phase structures as a result of first-order phase transitions.

Antiferromagnets with spin $S = 1/2$ on kagome and hyper-kagome lattices are rare substances, exotic structure–electronic states of matter. Scientists hope that these materials will find important applications. According to Hopkinson *et al.* (2007), excitement about such spin systems has also led to developments in mesoscopics (Wang *et al.*, 2006), optical lattices (Lowenstein, 2006; Wessel & Troyer, 2005) and computing (Osborne & Verstraete, 2006). One can expect new and interesting physical properties of solid solutions based on $Na_4Ir_3O_8$ and ordered (type 1:3) spinels under pressure and in magnetic fields. One of the main results of our theoretical studies is a significant increase of the structural types of substances for further research.

Acknowledgements

The authors thank the anonymous referees for valuable remarks that helped to improve the manuscript. We are also very grateful to Professor Dr W. F. Kuhs for his kind interest and encouragement. Some results of this work were obtained with the support of the Ministry of Education and Science of the Russian Federation in the framework of the State Task [Talanov, V. M., project N2983 (9.14)] and some were obtained with the financial support of the Ministry of Education and Science of the Russian Federation (Talanov, M.V., Federal program: state contract No. 14.575.21.0007; theme Nos. 213.01-11/2014-21, 3.1246.2014/K, 213.01-2014/012-ВГ).

References

Ahman, J., Svensson, G. & Albertson, J. (1996). *Acta Chem. Scand.* **50**, 391–394.
Aleksandrov, K. S. & Beznosikov, B. V. (2004). *Perovskites: Present and Future. Variety of Parent Phases, Phase Transitions, Possibilities of Synthesis of New Compounds.* Novosibirsk: Sib. Otd. Rus. Akad. Nauk.
Anderson, P. W. (1956). *Phys. Rev.* **102**, 1008–1013.
Arnold, V. I. (1992). *Catastrophe Theory*, 3rd ed. Berlin: Springer-Verlag.
Bauer, E. & Sigrist, M. (2012). Editors. *Non-Centrosymmetric Superconductors: Introduction and Overview.* Lecture Notes in Physics, Vol. 847. Berlin: Springer.
Bauer, J. & Bars, O. (1983). *J. Less-Common Met.* **95**, 267–274.
Bayer, G. (1967). *J. Less-Common Met.* **12**, 326–328.
Bergholtz, E. J., Laüchli, A. M. & Moessner, R. (2010). *Phys. Rev. Lett.* **105**, 237202.
Blasse, G. (1966). *J. Phys. Chem. Solids*, **102**, 383–389.
Bostrom, M. & Lidin, S. (2002). *J. Solid State Chem.* **166**, 53–57.
Boyko, T. D., Zvoriste, C. E., Kinski, I., Riedel, R., Hering, S., Huppertz, H. & Moewes, A. (2011). *Phys. Rev. B*, **84**, 085203.
Bramwell, S. T. & Gingras, M. J. P. (2001). *Science*, **294**, 1495–1501.
Catalan, G. & Scott, J. F. (2007). *Nature (London)*, **448**, E4–E5.
Chen, G. & Balents, L. (2008). *Phys. Rev. B*, **78**, 094403.

Chen, J., Greenblatt, M. & Waszczak, J. V. (1986). *J. Solid State Chem.* **64**, 240–248.
Datta, R. K. & Roy, R. (1963). *J. Am. Ceram. Soc.* **46**, 388–390.
Dekkers, M., Rijnders, G. & Blank, D. H. A. (2007). *Appl. Phys. Lett.* **90**, 021903.
Dvorak, V. (1978). *Czech. J. Phys.* B**28**, 989–994.
Ederer, C. & Spaldin, N. A. (2004). *Nat. Mater.* **3**, 849–851.
Eibenstein, U. & Jung, W. (1997). *J. Solid State Chem.* **133**, 21–24.
Ezikian, V. I., Ereyskaya, G. P., Talanov, V. M. & Hodarev, O. N. (1988). *Electrochimiya*, **24**, 1599–1604.
Giauque, W. F. & Ashley, M. (1933). *Phys. Rev.* **43**, 81–82.
Giauque, W. F. & Stout, J. W. (1936). *J. Am. Chem. Soc.* **58**, 1144–1150.
Gieck, C., Derstroff, V., Block, T., Felser, C., Regelsky, G., Jepsen, O. Ksenofontov, V., Gütlich, P., Eckert, H. & Tremel. W. (2004). *Chem. Eur. J.* **10**, 382–391.
Gorjaga, A. N., Talanov, V. M. & Borlakov, K. S. (1990). *Multiferroic Substances*, pp. 79–85. Moscow: Nauka.
Greedan, J. E., Raju, N. P., Wills, A. S., Morin, C. & Shaw, S. M. (1998). *Chem. Mater.* **10**, 3058–3067.
Griend, D. A. V., Boudin, S., Caignaert, V., Poeppelmeier, K. R., Wang, Y., Dravid, V. P., Azuma, M., Takano, M., Hu, Z. & Jorgensen, J. D. (1999). *J. Am. Chem. Soc.* **121**, 4787–4792.
Gufan, Yu. M. (1971). *Phys. Solid State*, **13**, 225–230.
Gufan, Yu. M. (1982). *Structural Phase Transitions.* Moscow: Nauka.
Hagemann, I. S., Huang, Q., Giao, X. P. A., Ramirez, A. P. & Cava, R. J. (2001). *Phys. Rev. Lett.* **86**, 894–897.
Hastings, J. M. & Corliss, L. M. (1962). *Phys. Rev.* **126**, 556–565.
Hemberger, J., Lunkenheimer, P., Fichtl, R., Krug von Nidda, H.-A., Tsurkan, V. & Loidl, A. (2005). *Nature (London)*, **434**, 364–367.
Hopkinson, J. M., Isakov, S. V., Kee, H.-Y. & Kim, Y. B. (2007). *Phys. Rev. Lett.* **99**, 037201.
Iwasaki, M., Takizawa, H., Uheda, K. & Endo, T. (2002). *J. Mater. Chem.* **12**, 1068–1070.
Jeanneau, E., Audebrand, N. & Louër, D. (2002). *Chem. Mater.* **14**, 1187–1194.
Johnston, D. C., Prakash, H., Zachariasen, W. H. & Viswanathan, R. (1973). *Mater. Res. Bull.* **8**, 777–784.
Joubert, J. C. & Durif, A. (1961). *Bull. Soc. Fr. Miner. Cristallogr.* **86**, 92.
Joubert, J. C. & Durif, A. (1964*a*). *Bull. Soc. Fr. Miner. Cristallogr.* **87**, 517–519.
Joubert, J. C. & Durif, A. (1964*b*). *Bull. Soc. Fr. Miner. Cristallogr.* **87**, 47–49.
Joubert, J. C. & Durif, A. (1964*c*). *C. R. Acad. Sci.* **258**, 4482–4485.
Kanno, R., Kawamoto, Y., Takeda, Y., Haregawa, M., Yamamoto, O. & Kinomura, N. (1992). *J. Solid State Chem.* **96**, 397–407.
Kanno, R., Takeda, Y., Takahashi, A., Yamamoto, O., Suyama, R. & Koizumi, M. J. (1987). *J. Solid State Chem.* **71**, 196–204.
Kanno, R., Takeda, Y. & Yamamoto, O. (1981). *Mater. Res. Bull.* **16**, 999–10058.
Kawai, H., Tabuchi, M., Nagata, M., Tukamoto, H. & West, A. R. (1998). *J. Mater. Chem.* **8**, 1273–1280.
Kim, J.-H., Myung, S.-T., Yoon, C. S., Kang, S. G. & Sun, Y.-K. (2004). *Chem. Mater.* **16**, 906–914.
King, R. B. (1987). *J. Solid State Chem.* **71**, 233–236.
Kovalev, O. V. (1993). *Representations of Crystallographic Space Groups. Irreducible Representations, Induced Representations and Co-representations*, edited by H. T. Stokes & D. M. Hatch, p. 349. London: Taylor and Francis Ltd.
Krupichka, S. (1976). *Physics of Ferrites and Related Magnetic Oxides*, Vol. 1, p. 355. Moscow: Mir.
Kuriyama, H., Matsuno, J., Niitaka, S., Uchida, M., Hashizume, D., Nakao A., Sugimoto, K., Ohsumi, H., Takata, M. & Takagi, H. (2010). *Appl. Phys. Lett.* **96**, 182103.
Kut'in, E. I., Lorman, V. L. & Pavlov, S. V. (1991). *Sov. Usp. Fizicheskikh Nauk.* **34**, 497–514.
Landau, L. D. & Lifshitz, E. M. (1980). *Statistical Physics*, Part 1. Oxford: Pergamon.
Lawler, M. J., Kee, H.-Y., Kim, Y. B. & Vishwanath, A. (2008). *Phys. Rev. Lett.* **100**, 227201.
Lawler, M. J., Paramekanti, A., Kim, Y. B. & Balents, L. (2008). *Phys. Rev. Lett.* **101**, 197202.
Lee, K.-W. & Picket, W. E. (2005). *Phys. Rev. B*, **72**, 174505.
Lee, P. A. (2008). *Science*, **321**, 1306–1307.
Lee, Y. J., Park, S. H., Eng, C., Parise, J. B. & Grey, C. P. (2002). *Chem. Mater.* **14**, 194–205.
Levanyuk, A. P. & Sannikov, D. G. (1971). *J. Exp. Theor. Phys.* **60**, 1109–1116.
Lifshitz, E. M. (1941). *J. Exp. Theor. Phys.* **41**, 255–268.
Lowenstein, M. (2006). *Nat. Phys.* **2**, 309–310.
Lutz, H. D., Partik, M., Schneider, M. & Wickel, Ch. (1997). *Z. Kristallogr.* **212**, 418–422.
Lutz, H. D., Pfitzner, A., Schmidt, W., Riedel, E. & Prick, D. (1989). *Z. Naturforsch. Teil A*, **44**, 756–758.
Lutz, H. D., Schmidt, W. & Haeuseler, H. (1985). *J. Solid State Chem.* **56**, 21–25.
McDaniel, C. L. (1974). *J. Solid State Chem.* **9**, 139–146.
Marin S. J., O'Keeffe, M. & Partin, D. E. (1994). *J. Solid State Chem.* **113**, 413.
Menyuk, N., Dwight, K. & Wold, A. (1964). *J. Phys. (Paris)*, **25**, 528–536.
Moessner, R. & Chalker, J. (1998). *Phys. Rev. Lett.* **80**, 2929–2932.
Mukovnin, A. A. & Talanov, V. M. (2014). *Eur. Phys. J. B*, **87**, 341–349.
Nageswara Rao, E. & Ghose, J. (1986). *Mater. Res. Bull.* **21**, 55–60.
Norman, M. R. & Micklitz, T. (2010). *Phys. Rev. B*, **81**, 024428.
Nunez-Regueiro, M. D., Lacroix, C. & Canals, B. (1996). *Phys. Rev. B*, **54**, 736–739.
Obradors, X., Labarta, A., Isalgu, A. Tejada, J., Rodriguez, J. & Pernet, M. (1988). *Solid State Commun.* **65**, 189–192.
Okamoto, Y., Nohara, M., Aruga-Katori, H. & Takagi H. (2007). *Phys. Rev. Lett.* **99**, 137207.
Osborne, T. J. & Verstraete, F. (2006). *Phys. Rev. Lett.* **96**, 220503.
Pati, S. K. & Rao, C. N. R. (2008). *Chem. Commun.* pp. 4683–4693.
Pauling, L. (1935). *J. Am. Chem. Soc.* **57**, 2680–2684.
Plumier, R. (1967). *J. Appl. Phys.* **39**, 635–636.
Podolsky, D. & Kim, Y. B. (2011). *Phys. Rev. B*, **83**, 054401.
Podolsky, D., Paramekanti, A., Kim, Y. B. & Senthil, T. (2009). *Phys. Rev. Lett.* **102**, 186401.
Poston, T. & Stewart, I. (1978). *Catastrophe Theory and its Applications.* London, San Francisco, Melbourne: Pitman.
Prokhorov, A. M., Gufan, Yu. M., Larin, E. S., Rudashevsry, E. G. & Shirokov, V. B. (1984). *Dokl. Akad. Nauk SSSR*, **227**, 1369.
Pröpper, D., Yaresko, A. N., Larkin, T. I., Stanislavchuk, T. N., Sirenko, A. A., Takayama, T., Matsumoto, A., Takagi, H., Keimer, B. & Boris, A. V. (2014). *Phys. Rev. Lett.* **112**, 087401.
Ramirez, A. P., Espinosa, G. P. & Cooper, A. S. (1990). *Phys. Rev. Lett.* **64**, 2070–2073.
Ramirez, A. P., Espinosa, G. P. & Cooper, A. S. (1992). *Phys. Rev. B*, **45**, 2505–2508.
Reeves, N., Pasero, D. & West, A. R. (2007). *J. Solid State Chem.* **180**, 1894–1901.
Reeves-McLaren, N., Smith, R. I. & West, A. R. (2011). *Chem. Mater.* **23**, 3556–3563.
Robbins, M., Willens, R. H. & Miller, R. C. (1967). *Solid State Commun.* **5**, 933–934.
Sakhnenko, V. P. & Talanov, V. M. (1979). *Sov. Phys. Solid State*, **21**, 2435–2444.
Sakhnenko, V. P. & Talanov, V. M. (1980). *Sov. Phys. Solid State*, **22**, 785–792.
Sahnenko, V. P., Talanov, V. M. & Chechin, G. M. (1986). *Fiz. Met. Metalloved.* **62**, 847–856.
Sellberg, B. & Rundqvist, S. (1965). *Acta Chem. Scand.* **19**, 760–762.
Shirokov, V. B. (2011). *Crystallogr. Rep.* **56**, 475–476.
Singh, D. J., Blaha, P., Schwarz, K. & Mazin, I. I. (1999). *Phys. Rev. B*, **60**, 16359.

Steinikeb, U. & Wallis, B. (1997). *Cryst. Res. Technol.* **32**, 187–193.
Stokes, H. T. & Hatch, D. M. (2007). *ISOTROPY*. http://stokes.byu.edu/iso/isotropy.html.
Stokes, H. T., Kisi, E. H., Hatch, D. M. & Howard, C. J. (2002). *Acta Cryst.* B**58**, 934–938.
Strobel, P., Ibarra-Palos, A., Anne, M. & Le Crisci, A. (2000). *J. Mater. Chem.* **10**, 429–436.
Strobel, P., Ibarra-Palos, A., Anne, M., Poinsignon, C. & Crisci, A. (2003). *Solid State Sci.* **5**, 1009–1018.
Sun, C. P., Huang, C. L., Lin, C. C., Her, J. L., Ho, C. J., Lin, J.-Y., Berger, H. & Yang, H. D. (2010). *Appl. Phys. Lett.* **96**, 122109.
Sun, C. P., Lin, C. C., Her, J. L., Ho, C. J., Taran, S., Berger, H., Chaudhuri, B. K. & Yang, H. D. (2009). *Phys. Rev. B*, **79**, 214116.
Takayama, T., Matsumoto, A., Nuss, J., Yaresko, A., Ishii, K., Yoshida, M., Mizuki, J. & Takagi, H. (2001). arXiv:1311.2885.
Talanov, V. M. (1996*a*). *Crystallogr. Rep.* **44**, 929–946.
Talanov V. M. (1996*b*). *Acta Cryst.* A**52**, C341.
Talanov, V. M. (2007). *Phys. Chem. Glass*, **33**, 852–870.
Talanov, V. M. & Ereyskaya, G. P. (2014). *Fundamentals of Nanochemistry and Nanotechnology*, edited by V. M. Talanov. Novocherkassk: South-Russian State Polytechnical University.
Talanov, V. M., Ereyskaya, G. P. & Yuzyuk, Y. I. (2008). *Introduction to Chemistry and Physics of Nanostructures and Nanostructured Materials*, edited by V. M. Talanov. Moscow: Academy of Natural Science.
Talanov, V. M. & Mukovnin, A. A. (2013). *Eur. Phys. J. B*, **86**, 448.
Talanov, V. M. & Paschenko, N. V. (1995). *Kristallographiya*, **40**, 982–988.
Talanov, V. M. & Shirokov, V. B. (2012). *Acta Cryst.* A**68**, 595–606.
Talanov, V. M. & Shirokov, V. B. (2013*a*). *Kristallographiya*, **58**, 296–301.
Talanov, V. M. & Shirokov, V. B. (2013*b*). *Crystallogr. Rep.* **58**, 314–318.
Talanov, V. M. & Shirokov, V. B. (2014). *Acta Cryst.* A**70**, 49–63.
Talanov, V. M., Shirokov, V. B., Ivanov, V. B. & Talanov, M. V. (2013). *Kristallographiya*, **58**, 80–91.
Talanov, V. M., Shirokov, V. B., Ivanov, V. V. & Talanov, M. V. (2015). *Crystallogr. Rep.* **60**, 101–110.
Talanov, V. M., Shirokov, V. B., Torgashev, V. I., Berger, G. A. & Burtsev, V. A. (2007). *Phys. Chem. Glass*, **33**, 822–834.
Tarte, P. & Collongues, R. (1964). *Ann. Chim.* **9**, 135–141.
Tashmetov, M. Yu., Em, V. T., Lee, C. H., Choi, Y. N., Lee, J. S., Shekhtman, V. Sh. & Dolukhanyan, S. K. (2005). *Physica B*, **369**, 254–260.
Thackeray, M. M. (1997). *Prog. Solid State Chem.* **25**, 1–71.
Todea, A. M., Merca, A., Bogge, H., Slageren, J., Dressel, M., Engelhardt, L., Luban, M., Glaser, T., Henry, M. & Muller, A. (2007). *Angew. Chem. Int. Ed.* **119**, 6218–6222.
Toledano, J.-C. & Toledano, P. (1987). *The Landau Theory of Phase Transitions.* Singapore: World Scientific.
Toledano, P. & Dmitriev, V. P. (1996). *Reconstructive Phase Transitions: in Crystals and Quasicrystals.* Singapore: World Scientific.
Torgashev, V. I. & Latush, L. T. (1997). *Kristallographiya*, **42**, 696–710.
Torgashev, V. I., Prokhorov, A. S., Komandin, G. A., Zhukova, E. S., Anzin, V. B., Talanov, V. M., Bush, A. A., Dressel, M. & Gorshunov, B. P. (2012). *Phys. Solid State*, **C54**, 330–339.
Townsend, M. O., Longworth, G. & Roudaut, E. (1986). *Phys. Rev. B*, **33**, 4919–4926.
Van der Biest, O. & Thomas, G. (1975). *Acta Cryst.* A**31**, 70–76.
Vandenberghe, R. E., Legrand, E., Scheerlinck, D. & Brabers, V. A. M. (1976). *Acta Cryst.* B**32**, 2796–2798.
Villain, J., Bidaux, R., Carton, J.-P. & Conte, R. (1980). *J. Phys. (Paris)*, **41**, 1263–1272.
Wang, L., Li, H., Huang, X. & Baudrin, E. (2011). *Solid State Ionics*, **193**, 32–38.
Wang, R. F., Nisoli, C., Freitas, R. S., Li, J., McConville, W., Cooley, B. J., Lund, M. S., Samarth, N., Leighton, C., Crespi, V. H. & Schiffer, P. (2006). *Nature (London)*, **439**, 303–306.
Wessel, S. & Troyer, M. (2005). *Phys. Rev. Lett.* **95**, 127205.
Yamasaki, Y., Miyasaka, S., Kaneko, Y., He, J.-P., Arima, T. & Tokura, Y. (2006). *Phys. Rev. Lett.* **96**, 207204.
Zhou, Y., Lee, P. A., Ng, T.-K. & Zhang, F.-C. (2008). *Phys. Rev. Lett.* **101**, 197201.
Zhu, Q., Sheng, T., Fu, R., Tan, C., Hu, S. & Wu, X. (2010). *Chem. Commun.* **46**, 9001–9003.